Precambrian Research 365 (2021) 106366

Contents lists available at ScienceDirect

Precambrian Research

journal homepage: www.elsevier.com/locate/precamres

Systematics of detrital zircon U–Pb ages from Cambrian–Lower Devonian rocks of northern Morocco with implications for the northern Gondwanan passive margin

Cristina Accotto [a,*], David Martínez Poyatos [a], Antonio Azor [a], Cristina Talavera [b], Noreen J. Evans [c], Antonio Jabaloy–Sánchez [a], Abdelfatah Tahiri [d], Hassan El Hadi [e], Ali Azdimousa [f]

[a] Department of Geodynamics, University of Granada, Granada, Spain
[b] School of Geosciences, University of Edinburgh, Edinburgh, UK
[c] School of Earth and Planetary Sciences, John the Laeter Centre, Curtin University, Perth, Australia
[d] Laboratory of Geo–biodiversity and Natural Patrimony (GEOBIO), Scientific Institute, Geophysics, Natural Patrimony and Green Chemistry Research Center (GEOPAC), Mohammed V University, Rabat, Morocco
[e] Laboratory of Geodynamics of Ancient Belts, Faculty of Science Ben M'Sik, Hassan II University, Casablanca, Morocco
[f] Faculté Pluridisciplinaire de Nador et Laboratoire des Géosciences Appliquées, Faculté des Sciences, Université Mohammed I, Oujda, Morocco

ARTICLE INFO

Keywords:
NW African Variscides
Moroccan Mesetas
West African Craton
Northern Gondwanan margin
Provenance study
Cambrian rifting

ABSTRACT

The systematic acquisition of U–Pb geochronological data from detrital zircon grains has become an essential tool in tectonic studies focused on reconstructing the pre–Variscan geography of the northern Gondwanan passive margin. New detrital zircon ages for 16 samples from the Cambrian–Lower Devonian succession of the Moroccan Mesetas (northern Morocco) are reported here. The results, combined with previously published data, reassert the strong West African Craton affinity of the Paleozoic sedimentary rocks, characterized by dominant Cadomian/Pan–African (*c.* 850–540 Ma) and Eburnean (*c.* 2.2–1.9 Ga) detrital zircon populations and a minor Leonian/Liberian (*c.* 2.5 Ga) population. Primary sources of these zircon grains are well established as the West African Craton located just to the south, but also in the Precambrian basement that locally crops out in the Moroccan Mesetas themselves. During the Cambrian–Early Ordovician, erosion preferentially dismantled Cadomian (*c.* 590–540 Ma) arc–derived rocks of the Gondwanan continental margin, while later, the slightly older Pan–African (*c.* 650–600 Ma) basement became the main sediment source. In the studied samples, irregularly present minor detrital zircon populations suggest additional sediment provenance from secondary sources such as: (i) remote northeastern African cratons (*e.g.*, Saharan Metacraton and/or Arabian–Nubian Shield) that likely could have provided the *c.* 1.1–0.9 Ga and, possibly, the *c.* 1.9–1.7 Ga zircon grains, and (ii) rift–related Cambrian–Early Ordovician volcanic centers in the Moroccan Mesetas that supplied heterogeneously distributed – although locally dominant in small areas – sedimentary detritus before rift abortion and burial underneath the overlying passive margin sedimentary succession.

1. Introduction

The systematic U–Pb dating of detrital zircon grains is a powerful tool that, in the last decades, has been widely applied in sediment provenance studies and paleogeographic reconstructions (*e.g.*, Fedo et al., 2003; Gehrels, 2012). These studies have been fundamental in the recognition of the terranes involved in pre–Alpine orogenies, whose present–day field relationships are often complex and/or obliterated by superposed tectonics. In Europe, detrital zircon geochronology formed the basis of a good number of studies (*e.g.*, Braid et al., 2011; Eckelmann et al., 2014; Fernández-Suárez et al., 2014; Franke and Dulce, 2017; Gutiérrez-Alonso et al., 2015; Linnemann et al., 2004; Nance et al., 2008; Pereira et al., 2017; Pereira et al., 2012; Pérez-Cáceres et al., 2017; Shaw et al., 2014) and provided a better understanding of the late Paleozoic Variscan belt. The Variscan orogen formed by the closure of the Rheic Ocean and the subsequent collision between the Gondwanan

* Corresponding author.
E-mail address: accotto@ugr.es (C. Accotto).

https://doi.org/10.1016/j.precamres.2021.106366
Received 14 June 2021; Received in revised form 18 August 2021; Accepted 18 August 2021
Available online 9 September 2021

and the Laurussian supercontinents, involving several minor peri–Gondwanan terranes (*e.g.*, Franke et al., 2017; Matte, 2001; Simancas et al., 2005).

The southward along–strike extension of the European Variscan belt, partially obliterated by younger orogenic systems (*e.g.*, Alpine Betic–Rif belt, Fig. 1A), crops out in northern Morocco and western Mauritania. In Morocco, the areas affected by the Variscan orogeny are collectively referred to as the "Moroccan Variscides", and have been mainly investigated from stratigraphic and tectonic points of view (*e.g.*, El Hassani et al., 2003; Hoepffner et al., 2006; Michard, 1976; Michard et al., 2010b; Michard et al., 2010a; Michard et al., 1989; Pique, 1994; Piqué, 2001; Piqué, 1981; Piqué and Michard, 1989; Simancas et al., 2009; Simancas et al., 2005; Tahiri, 1991; Villeneuve et al., 2010; Walliser et al., 2000; Walliser et al., 1995). The use of detrital zircon geochronological data has been recently incorporated into the study of this part of the Variscan belt (Abati et al., 2010; Accotto et al., 2019; Accotto et al., 2020; Accotto et al., 2021; Accotto et al., in press; Avigad et al., 2012; El Houicha et al., 2018; Gärtner et al., 2017; Gärtner et al., 2018; Ghienne et al., 2018; Letsch et al., 2018; Pérez-Cáceres et al., 2017). Nevertheless, most of these works are focused on very localized areas, while most sectors remain unsampled. Furthermore, a regional–scale correlation among samples, especially for lower–middle Paleozoic rocks, is still missing.

The northern Moroccan Variscides are traditionally divided into several domains (Fig. 1B) separated by fault zones, whose paleogeographic importance is still a matter of debate (*e.g.*, Hoepffner et al., 2006; Michard et al., 2010a; Michard et al., 2010b; Simancas et al., 2009; Simancas et al., 2010). These domains are: the Caledonian Sehoul Block, the Western Moroccan Meseta (WMM), subdivided into Coastal Block, Central Zone and Nappe Zone (see Section 2.1), the Eastern Moroccan Meseta (EMM; see Section 2.2), the Southern Zone, and the Anti-Atlas foreland. With the exception of the Sehoul Block, all of the domains of the northern Moroccan Variscides are considered to have belonged to the northern Gondwanan passive margin during Cambrian–Early Devonian times. This is based on stratigraphic similarities and the absence of ophiolite and/or high–pressure metamorphic belts separating the different domains (*e.g.*, Michard et al., 2010b; Simancas et al., 2005). In this context, systematic geochronological detrital zircon studies are an important tool to decipher putative differences between the domains and shed light on the paleogeographic importance of their tectonic boundaries, *i.e.*, their influence on the source to sink detrital sediment routing systems.

In this study, we collected 16 upper Cambrian–Lower Devonian (meta)sandstone samples from different areas of the Moroccan Mesetas (WMM and EMM; Fig. 1) and carried out U–Pb geochronological analyses on detrital zircon grains in order to investigate the detrital sources that controlled the sedimentation in this part of the northern Gondwanan passive margin. To do so, we have also considered previously published data on other coeval samples of the region, as listed in Table 1.

2. Geological setting

2.1. The Western Moroccan Meseta

The igneous Paleoproterozoic–Ediacaran basement of the northern Moroccan Variscides (Fig. 1) crops out locally in the WMM at El Jadida (Coastal Block; El Haibi et al., 2020; El Houicha et al., 2018), Tiflet (Central Zone; El Haïbi et al., 2021; Tahiri et al., 2010), Rehamna (Central Zone; Baudin et al., 2003; Pereira et al., 2015), and Goaïda areas (Nappe Zone; Ouabid et al., 2017). The unconformable Cambrian–Lower Devonian sedimentary succession is represented by siliciclastic passive margin deposits, locally intruded by Cambrian–Ordovician magmatic rocks (Pouclet et al., 2018, and references therein), and followed by a Devonian mainly carbonatic sequence. Local differences are shown in Fig. 2 and described in the following subsections. After Late Devonian time, the synorogenic succession mainly comprises siliciclastic turbiditic rocks with a few carbonatic intercalations of early Carboniferous age. Unconformable late Carboniferous–Permian sedimentary sequences deposited in continental basins developed locally. The Paleozoic succession was intruded by upper Carboniferous–Permian Variscan dykes and granitoids (*e.g.*, El Hadi et al., 2006a, and references therein; Kharbouch, 1994; Kharbouch et al., 1985), and unconformably overlain by post–orogenic Triassic volcano–sedimentary rocks (Destombes, 1987).

The Paleozoic succession of the WMM was deformed by late Carboniferous Variscan folding, coeval to low– to very low–grade metamorphism (Hoepffner et al., 2005; Michard et al., 2010b).

2.1.1. The Coastal Block

The Cambrian succession of the Coastal Block is characterized by siliciclastic deposits locally intruded by basalts and andesites (*e.g.*, Oued Rhebar – *c.* 40 km SW of Rabat – and Sidi Saïd Maâchou – *c.* 35 km E of El Jadida – volcanic centers; Pouclet et al., 2018, and references therein). The siliciclastic succession records an increase of grain size from a predominance of shales in the early–middle Cambrian ("*Schistes à Paradoxides*") to mainly sandy sediments, which culminate in late Cambrian with the deposition of a thick and continuous level of quartzitic microconglomeratic sandstones and arkoses ("El Hank" Formation; Fig. 2; Cailleux, 1994, and references therein; Destombe and Jeannette, 1966). The base of the Ordovician is marked by a transgression. After a basal level of conglomerates and greywackes, the succession is mainly characterized by shales with an increase of sandy and microconglomeratic layers deposited at middle–late Ordovician time (Destombe and Jeannette, 1966; Ouanaimi et al., 2016). The Silurian succession is very similar in all of the Moroccan Mesetas and characterized by black shales with graptolites (Destombe and Jeannette, 1966; Zahraoui, 1994, and references therein). A particularity of the Coastal Block is the presence of a few carbonatic layers, which are more common upwards and appear interbedded with the shales. The deposition of shale continued during the Early Devonian with an increase in carbonatic beds, indicating the establishment of a carbonatic platform in this part of the Gondwanan passive margin.

2.1.2. The Central Zone

No Cambrian rocks have been dated until now in the studied areas of the Central Zone (Oued Akreuch, Ezzhiliga and Oulmes areas). The Paleozoic succession (Fig. 2) started with the deposition of Ordovician shales with sandy and/or conglomeratic intercalations, more common during the Middle–Late Ordovician (*e.g.*, El Hassani, 1991; Tahiri and El Hassani, 1994). In the northwestern sector of this zone, close to the Coastal Block (*e.g.*, Oued Akreuch area), basaltic and gabbroic intercalations are also common (El Hadi et al., 2014; El Hassani, 1991, and references therein). The Silurian is represented by black shales with graptolites and carbonatic beds, which are more common in late Silurian time (El Hassani, 1991, and references therein). The Lower Devonian deposition records the establishment of a carbonatic platform in the western sectors (*e.g.*, Oued Akreuch area), and more subsiding conditions in the eastern sectors, which resulted in the prevalence of turbiditic deposits (*e.g.*, Ezzhiliga and Oulmes areas; Bhija et al., 1999; Razin et al., 2001; Tahiri, 1991, and references therein).

2.1.3. The Nappe Zone

The Nappe Zone corresponds to the easternmost part of the WMM, and is characterized by Variscan thrust tectonics (Michard et al., 2010b, and references therein), particularly in the eastern part of the zone (Azrou–Khenifra areas; Fig. 1C; Hoepffner et al., 2006).

To the southeast, the Khenifra nappe is made up of an upper Cambrian–Upper Ordovician succession of turbiditic shales, sandstones and subordinate conglomerates, followed by the Silurian black shales with graptolites and by Lower Devonian turbidites (Bouabdelli and Piqué, 1996).

In the Azrou area, three para–autochthonous units, characterized by

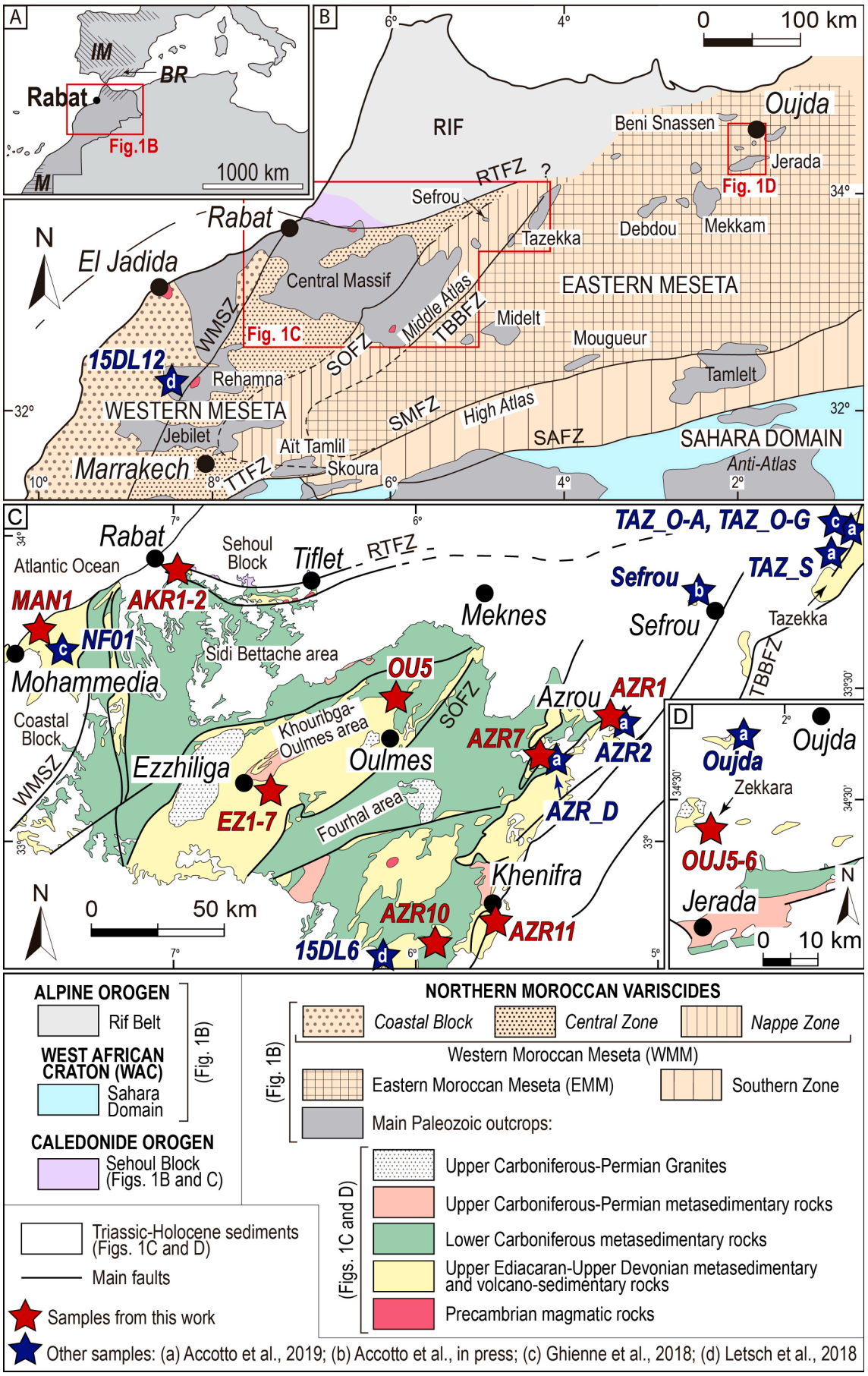

(caption on next page)

Fig. 1. Schematic geological maps of the Paleozoic inliers and structural domains in northern Morocco. A) Location of northern Morocco; IM. Iberian Massif; BR. Betic–Rif Belt; M: Mauritanides. B) Northern Moroccan Variscides (modified from Hoepffner et al., 2006; Michard et al., 2010b). C) Detail of the northern Western Moroccan Meseta (modified from Arboleya et al., 2004; Becker and El Hassani, 2020; Charriere, 1989). D) Detail of the Oujda–Zekkara area (modified from Muratet, 1995). RTFZ: Rabat–Tiflet Fault Zone; WMSZ: Western Meseta Shear Zone; SOFZ: Smaala–Oulmès Fault Zone; TBBFZ: Tazekka–Bsabis–Bekrit Fault Zone; TTFZ: Tizin'Test Fault Zone; SMFZ: South Meseta Fault Zone; SAFZ: South Atlas Fault Zone. Stars indicate the location of the samples studied in this work (in red) and other Cambrian–Lower Devonian samples already published (in blue; see references in the Figure legend).

Table 1
Previously published results used in this work.

Original sample code	Codes used in this work	Age	References
	COASTAL BLOCK		
15DL12	15DL12	upper Cambrian	Letsch et al. (2018)
NF01	NF01	Upper Ordovician	Ghienne et al. (2018)
	NAPPE ZONE (KHENIFRA AREA)		
15DL6	15DL6	upper Cambrian–Lower Ordovician	Letsch et al. (2018)
	NAPPE ZONE (AZROU AREA)		
AZR2	AZR2	Upper Ordovician	Accotto et al. (2019)
AZR4, AZR5, AZR6	AZR_D	Lower Devonian	
	NAPPE ZONE (SEFROU AREA)		
SF1, SF2, SF3	Sefrou	Lower–Upper Ordovician	Accotto et al. (in press)
	NAPPE ZONE (TAZEKKA AREA)		
TAZ2, TAZ3	TAZ_O-A	Upper Ordovician	Accotto et al. (2019)
TeB1, TeB2, TeB3, Tf1, Tf2, Tf3, Tf4, Tf5, Tf6	TAZ_O-G	Upper Ordovician	Ghienne et al. (2018)
TAZ5, TAZ6	TAZ_S	Silurian	Accotto et al. (2019)
	EASTERN MOROCCAN MESETA (OUJDA AREA)		
OUJ2, OUJ3	Oujda	Upper Ordovician	Accotto et al. (2019)

an Upper Ordovician–upper Carboniferous succession, are overlain by an allochthonous nappe of Lower–Upper Devonian rocks (see sketched structural relationships in Fig. 2; Bouabdelli et al., 1989). We only collected samples from the basal section of the Eastern (Upper Ordovician–lower Carboniferous) and Central (Lower Devonian–Visean) para–autochthonous units. The Eastern unit is characterized by Upper Ordovician turbiditic microconglomeratic to shaly rocks, followed by a monotonous succession of Silurian black shales. The increase of carbonatic layers interbedded with the shales marks the establishment of an Early Devonian carbonatic platform (Bouabdelli, 1982). In contrast, the corresponding Lower Devonian succession in the Central unit is characterized by siliciclastic deposits, while the carbonatic sedimentation started at Middle Devonian time (Walliser et al., 2000).

Towards the northeast, in the Sefrou and Tazekka areas, sedimentation was characterized by shales and sandstones throughout the Cambrian–Devonian period (Charriere, 1990, and references therein; Hoepffner, 1987, and references therein). There is no evidence of carbonatic sedimentation during the Silurian, although in the Sefrou area, the stratigraphic sequence is incomplete (Charriere, 1990). In the Imouzzer area, a few kilometers SW of Sefrou, Middle–Upper Devonian carbonatic olistoliths were observed (Charriere, 1990).

2.2. The Eastern Moroccan Meseta

The Paleozoic rocks of the EMM (Fig. 1B, D) crop out in relatively small inliers below the Mesozoic–Cenozoic cover. The lower Paleozoic succession is a monotonous succession of shales, sandstones, and greywackes (Fig. 2), attributed to the Cambrian–Ordovician (Desteucq and Fournier-Vinas, 1981; Hoepffner, 1989; Hoepffner, 1977; Rauscher et al., 1982), and overlain by Silurian black shales. The Lower Devonian is composed of siliciclastic sediments (mainly shales with a few sandy lenses that become more common during the Middle–Late Devonian and Tournaisian), representing a a deepening of the depositional environment, in contrast with the coeval carbonatic platform that characterized most of the WMM. An upper Visean–Kasimovian succession unconformably overlies the Famennian–Tournaisian rocks (Médioni, 1979, and references therein); this second synorogenic succession is constituted by upper Visean volcano–sedimentary layers followed by siliciclastic turbidites and continental (limnic facies) sediments (*e.g.*, Jerada area; Berkhli et al., 1999).

Variscan metamorphism in the EMM is generally of low– to very low–grade (except in the Midelt and northern Tamlet areas; Hoepffner, 1989) and deformation is variable: in some areas, the Paleozoic succession recorded both Eovariscan (intense recumbent folding) and Variscan (upright folding) deformational events (*e.g.*, Debdou–Mekkam areas; Accotto et al., 2020), while others were only affected by the Variscan tectonic phase (*e.g.*, Jerada, Oujda, Beni Snassen areas; Fig. 1B). The EMM was also intruded by upper Carboniferous–Permian granitoids (El Hadi et al., 2006a, and references therein).

3. Samples and methods

We collected 16 sandstone samples in different areas of the Western and Eastern Moroccan Mesetas (Fig. 1C and D). The location of the samples and other details are synthetized in Table 2. Age assignement (Fig. 2 and Table 2) is based on the geological data available in the sampling sites (local biostragraphic studies and/or geological maps; see specific references for each sample in Section 4).

Most of the samples are quartzites or quartzitic sandstones, with 90–99% of quartz grains of variable size: *c.* 0.05 mm in samples AKR1, EZ2, and AZR10, *c.* 0.1–0.3 mm in samples AKR1, AKR2, EZ1, EZ6, AZR10, and AZR1, and *c.* 0.4–1.0 mm in samples EZ4, EZ5, AZR10, and AZR7. The quartz grains are usually sub–rounded and muscovite and/or oxides can be observed in fractures or interstitial positions. Samples EZ7, OU5, and AZR11 are sandstones with abundant sub–rounded quartz grains (diameters varying between *c.* 0.05 and *c.* 0.25 mm) and abundant phyllosilicates and oxides. Finally, samples MAN 1, OUJ5, and OUJ6 are greywackes characterized by a fine–grained matrix, embedding *c.* 0.3–1.0 mm quartz grains, oxides, and phyllosilicates, as well as shale, sandstone, plagioclase, and volcanic fragments.

3.1. U–Pb analyses

Each sample consisted of *c.* 4–5 kg of rock, which was mechanically smashed with a jaw–crusher and sorted by sieving in the laboratories of the University of Granada (Spain). Zircon grains were separated from the 0.3–0.05 mm fraction using magnetic separation and, finally, handpicking. The grains were then mounted in epoxy discs, polished, cleaned, gold–coated, and imaged by cathodoluminescence (CL) using a Mira3 Field Emission SEM instrument at the John the Laeter Centre (JdLC) of the Curtin University (Perth, Australia) and a Carl Zeiss SIGMA HD VP Field Emission SEM at the School of GeoSciences of the University of Edinburgh (United Kingdom). A selection of CL images for each sample is presented in Appendix A, together with a brief description of the detrital zircon grains in each sample.

The U–Th–Pb analysis of most of the detrital zircon grains was

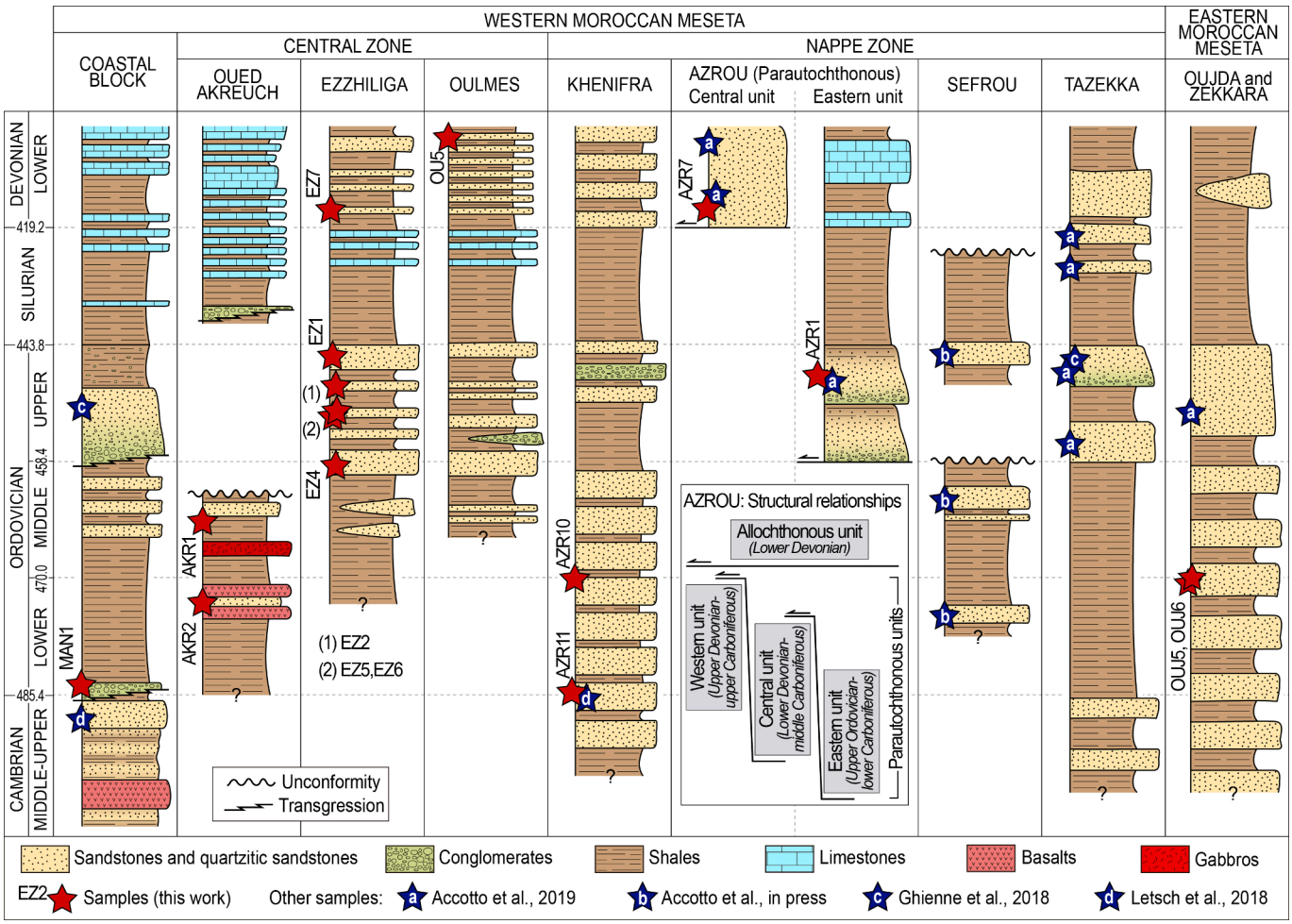

Fig. 2. Schematic stratigraphic columns of the middle Cambrian–Lower Devonian successions of the northern Moroccan Variscides cropping out in the studied areas (Bouabdelli et al., 1989; Cailleux, 1994; Charriere, 1990; Choubert et al., 1978; El Hassani, 1991; Hoepffner, 1989; Horon, 1952; Marhoumi et al., 1989; Razin et al., 2001; Tahiri, 1991; Tahiri, 1994; Vidal and Hoepffner, 1979). Stars indicate the approximate location of the studied samples (in red) and other samples already published (in blue; see references in the Figure legend). Not to scale.

performed at the JdLC GeoHistory Facility (Curtin University, Perth, Australia) using laser ablation inductively coupled plasma mass spectrometry (LA–ICPMS; Table 2). Nevertheless, because of the great variability of grain size in a few samples, sensitive high–resolution ion microprobe (SHRIMP) and secondary ion mass spectrometry (SIMS) techniques were performed (Table 2), at the JdLC and the University of Edinburgh, respectively. These analytical methods, standard zircons, and references to the methodologies are explained in Appendix B and the results can be found in Appendix C.

LA–ICPMS, SHRIMP, and SIMS results were then combined to yield a sufficient number of data for statistical analysis (Vermeesch, 2004). Discordance levels were calculated following Spencer et al. (2016) (see Appendix B), and data with levels exceeding ±10% were discarded.

The statistical analyses were performed on $^{206}Pb/^{238}U$ dates for ages younger than 1.5 Ga and $^{207}Pb/^{206}Pb$ dates for older grains (Spencer et al., 2016). Kernel Density Estimators (KDE) and histograms were prepared using the DensityPlotter 8.4 software (Vermeesch, 2012) and applying a KDE bandwidth and a histogram bin width of 30 Ma in graphs including all the data, or 5 Ma in diagrams showing only data in a limited time span (Figs. 3 and 4). Each detrital zircon population was defined by choosing age intervals that were statistically (*i.e.*, peaks in the KDE diagrams) and geologically (*i.e.*, ages of the main geological events; see legend in Fig. 1 and section 5 for discussion) meaningful. The mean ages of the populations were calculated using the mixture–modelling tool in DensityPlotter 8.4. All the errors are expressed at 1σ level. The youngest detrital zircon populations were calculated using the Isoplot software (Ludwig, 2003) taking into account the youngest cluster of at least 4 grains with overlapping 2σ uncertainties (Dickinson and Gehrels, 2009).

3.2. Hf isotopes analyses

Due to the peculiar U–Pb results obtained in sample AZR10 (see Section 4), Hf analyses were performed on the detrital zircon grains of this sample with concordant U–Pb results and sizes > 50 μm. These analyses were performed at the GeoHistory Facility, JdLC (Curtin University, Perth, Australia) using a Resonetics resolution M−50A excimer laser, coupled to a Nu Plasma II multi–collector inductively coupled plasma mass spectrometer (LA–MC–ICPMS). The detailed analytical methods, reference materials, data reduction, and references to the methodology are described in Appendix B. Full results are listed in Appendix D. Statistical analysis was performed using an Excel® worksheet and errors are expressed at 2σ level.

4. Results

4.1. El Mansouria area (Coastal Block, WMM)

One hundred and nineteen zircon grains from a lower Ordovician (Destombe, 1987) sample (MAN1) were analyzed by LA–ICPMS,

Table 2
List and details of the studied samples. (*) total number of analyses performed *vs* concordant results (in bold).

Sample	IGSN (IEACC)	Location (UTM, WGS84)			Lithology	Stratigraphic age	U-Pb geochronology	
		Zone	X (m E)	Y (m N)			Method	Analyses (*)
					COASTAL BLOCK (EL MANSOURIA AREA)			
MAN1	0040	29S	658014	3735681	Greywacke	Early Ordovician	LA-ICPMS	120/**109**
					OUED AKREUCH AREA			
AKR1	0038	29S	704231	3757672	Quartzitic sandstone	Middle Ordovician	LA-ICPMS	150/**124**
AKR2	0039	29S	704321	3757780	Quartzitic sandstone	Early Ordovician	LA-ICPMS	150/**130**
					EZZHILIGA AREA			
EZ1	0032	29S	733796	3682713	Quartzitic sandstone	Late Ordovician	LA-ICPMS	42/**30**
							SHRIMP	50/**36**
EZ2	0033	29S	733776	3682624	Quartzitic sandstone	Late Ordovician	LA-ICPMS	75/**68**
EZ4	0034	29S	737693	3682341	Quartzitic sandstone	Middle-Late Ordovician	LA-ICPMS	165/**156**
EZ5	0035	29S	737554	3682849	Quartzitic sandstone	Late Ordovician	LA-ICPMS	180/**167**
EZ6	0036	29S	739164	3684150	Quartzitic sandstone	Late Ordovician	LA-ICPMS	150/**135**
EZ7	0037	29S	735286	3683869	Quartzitic sandstone	Early Devonian	LA-ICPMS	99/**86**
							SIMS	40/**35**
					OULMES AREA			
OU5	0031	29S	777396	3715910	Sandstone	Early Devonian	LA-ICPMS	150/**135**
					KHENIFRA AREA			
AZR10	0029	30S	233758	3633628	Quartzitic sandstone	Early-Middle Ordovician	LA-ICPMS	120/**97**
AZR11	0030	30S	252046	3643326	Sandstone	Cambrian-Ordovician	LA-ICPMS	78/**67**
							SIMS	47/**44**
					AZROU AREA			
AZR1	0023	30S	295882	3705386	Quartzitic sandstone	Late Ordovician	LA-ICPMS	100/**90**
							SIMS	31/**31**
AZR7	0028	30S	271772	3695342	Quartzitic sandstone	Early Devonian	LA-ICPMS	168/**146**
					ZEKKARA AREA			
OUJ5	0021	30S	574362	3821747	Greywacke	Cambrian-Ordovician	LA-ICPMS	145/**143**
OUJ6	0022	30S	574362	3821747	Greywacke	Cambrian-Ordovician	LA-ICPMS	150/**144**

yielding 120 ages, 109 of which were concordant (Fig. 3A). The main detrital zircon age populations obtained in this sample are:

- Cambrian–Ordovician (*c.* 537–450 Ma, n = 40, 36.7% of the data) with a Cambrian mean age (506.6 ± 0.7 Ma) and peaks at *c.* 460, 505 (main peak) and 530 Ma.
- Cryogenian–Ediacaran (*c.* 660–551 Ma, n = 50, 45.9% of the data) with a late Ediacaran mean age (596.5 ± 0.8 Ma) and peaks at *c.* 575, 580 (main peak), 600, 630, and 660 Ma.
- Rhyacian–Orosirian (*c.* 2096–2010 Ma, n = 12, 11% of the data) with an early Orosirian mean age (2048.7 ± 5.0 Ma).

Scattered grains yielded middle Orosirian (n = 2, *c.* 1940 Ma) and Neoarchean–early Rhyacian (n = 5, *c.* 2720–2260 Ma) ages. The youngest detrital zircon population of this sample comprises 28 dates and yielded a middle Cambrian age (505.8 ± 0.9 Ma, MSWD = 0.95).

4.2. Oued Akreuch area (Central Zone, WMM)

Almost 150 LA–ICPMS analyses were carried out on detrital zircon grains from each Ordovician (El Hassani, 1991) sample from Oued Akreuch (143 grains in AKR1 and 149 grains in AKR2), yielding 124 and 130 concordant results, respectively (Table 2). The age distribution is statistically identical in both samples, and the results have been combined in Fig. 3B. The main detrital zircon age populations are as follows:

- Late Tonian–Ediacaran (*c.* 856–543 Ma, n = 125, 49.2% of the data) with a late Cryogenian (639.2 ± 0.4 Ma) mean age. Main peaks appear at *c.* 600, 635 and 650 Ma. Secondary peaks are at *c.* 550, 620, and 670 Ma, while dates between *c.* 856 and *c.* 706 Ma appear more scattered.
- Stenian–early Tonian (*c.* 1119–891 Ma, n = 22, 8.7% of the data) with an early Tonian mean age (974.3 ± 1.4 Ma).
- Orosirian–Statherian (*c.* 1929–1766 Ma, n = 19, 7.5% of the data) with a late Orosirian mean age (1836.0 ± 3.7 Ma).
- Rhyacian–Orosirian (*c.* 2188–1941 Ma, n = 53, 20.8% of the data) clustered in two peaks with Rhyacian (2143.5 ± 3.4 Ma) and early Orosirian (2018.1 ± 3.2 Ma) ages.
- Neoarchean–Siderian (*c.* 2770–2404 Ma, n = 19, 7.5% of the data) with a late Neoarchean mean age (2587.2 ± 2.9 Ma).

Scattered grains yielded Cambrian (*c.* 525–487 Ma, n = 2), Statherian–Ectasian (*c.* 1707–1200 Ma, n = 6), Rhyacian (*c.* 2366–2225 Ma, n = 7), and Paleoarchean (*c.* 3437 Ma, n = 1) ages. The youngest detrital zircon population of the two samples is late Ediacaran (549.6 ± 2.1 Ma, MSWD = 0.59) and comprises 5 dates.

4.3. Ezzhiliga area (Central Zone, WMM)

In this area, five Middle–Upper Ordovician samples and one Lower Devonian (Razin et al., 2001) sample were collected (Fig. 3C and D). Six hundred and sixty–two LA–ICPMS and SHRIMP analyses were carried out on a total of 628 zircon grains from the five Ordovician samples. Of these, 592 yielded concordant dates. All the Ordovician samples show statistically identical results and, accordingly, they have been plotted together (Fig. 3C). The following detrital zircon age populations have been found:

- Cambrian–Ordovician (*c.* 539–476 Ma, n = 16, 2.7% of the data) with a Cambrian mean age (519.9 ± 1.3 Ma) and a peak at *c.* 535 Ma.
- Late Tonian–Ediacaran (*c.* 853–541 Ma, n = 332, 56.1% of the data) with an Ediacaran mean age (627.0 ± 0.3 Ma) and a main peak at *c.* 620 Ma. Second–order peaks appear at *c.* 560, 590, 630, and 650 Ma, while data between *c.* 853 and *c.* 694 Ma are more scarce and scattered.

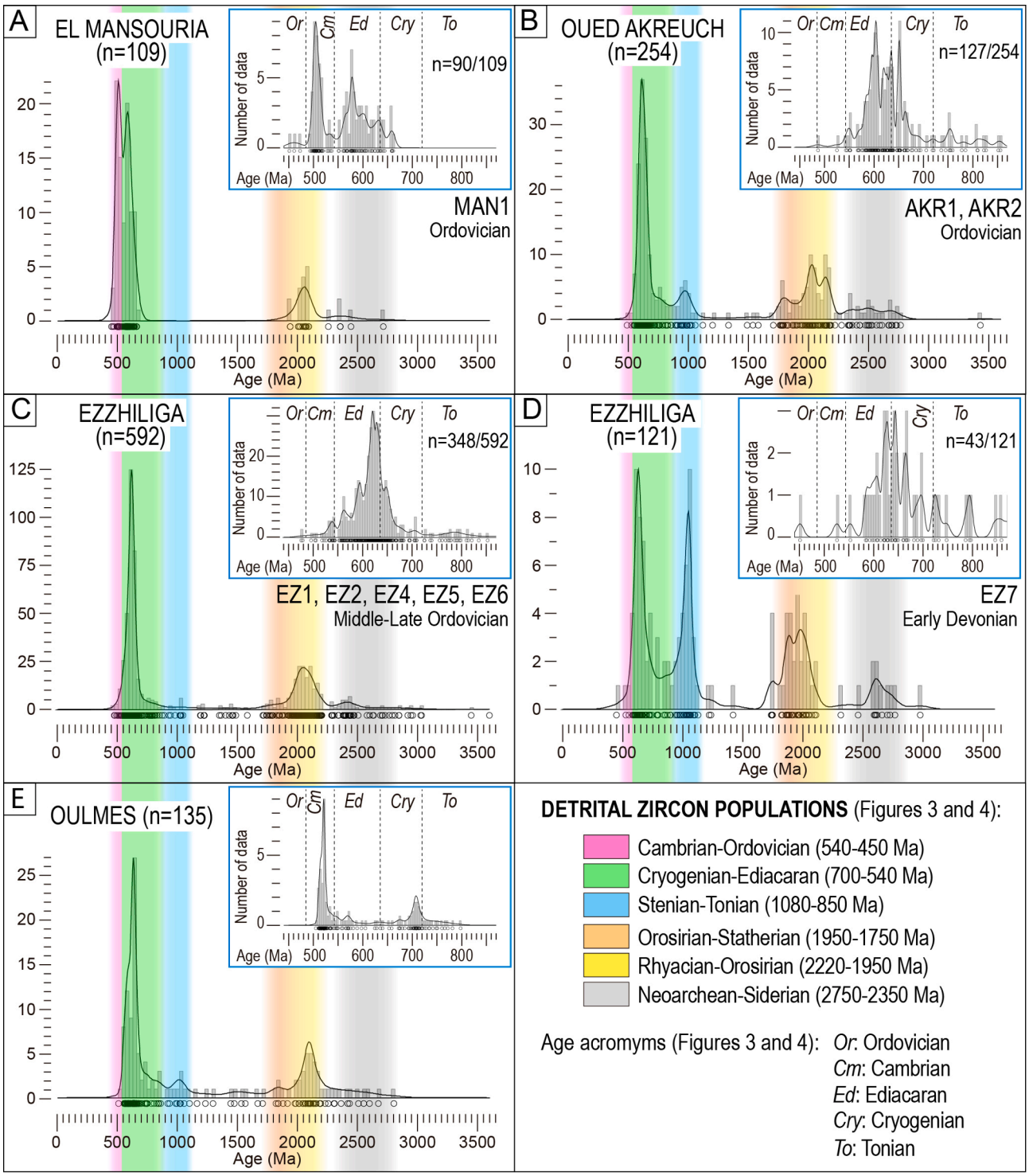

Fig. 3. KDE (black lines) and histograms (grey bars) showing the U–Pb results in the 0–3600 Ma and 440–870 Ma (in the blue boxes) intervals. (A) El Mansouria area (Coastal Block, WMM); (B) Oued Akreuch area (Central Zone, WMM); Ordvician (C) and Devonian (D) samples from Ezzhiliga area (Central Zone, WMM); (E) Oulmes area (Central Zone, WMM). Color bars indicate the most common detrital zircon populations recognized in all the samples.

- A very minor Stenian–Tonian population (*c.* 1049–875 Ma, n = 11, 1.9% of the data), mainly concentrated in samples EZ1, EZ5, and EZ6. The mean age is early Tonian (991.7 ± 2.3 Ma).
- Orosirian–Statherian (*c.* 1902–1716 Ma, n = 21, 3.5% of the data) with an early Statherian mean age (1815.8 ± 3.5 Ma).
- Rhyacian–Orosirian (*c.* 2210–1926 Ma, n = 150, 25.3% of the data) with a late Rhyacian mean age (2069.3 ± 1.1 Ma).
- Siderian–early Rhyacian (*c.* 2478–2291 Ma, n = 27, 4.6%) with a Siderian mean age (2411.7 ± 2.7 Ma).

Scattered grains in the Ordovician samples yielded Calymmian–-Stenian (*c.* 1584–1195 Ma, n = 14) and Archean (*c.* 3608–2514 Ma, n = 21) ages. The youngest detrital zircon population of the combined group of Ordovician samples is early Cambrian (534.4 ± 1.9 Ma, MSWD = 0.43) and includes 9 dates.

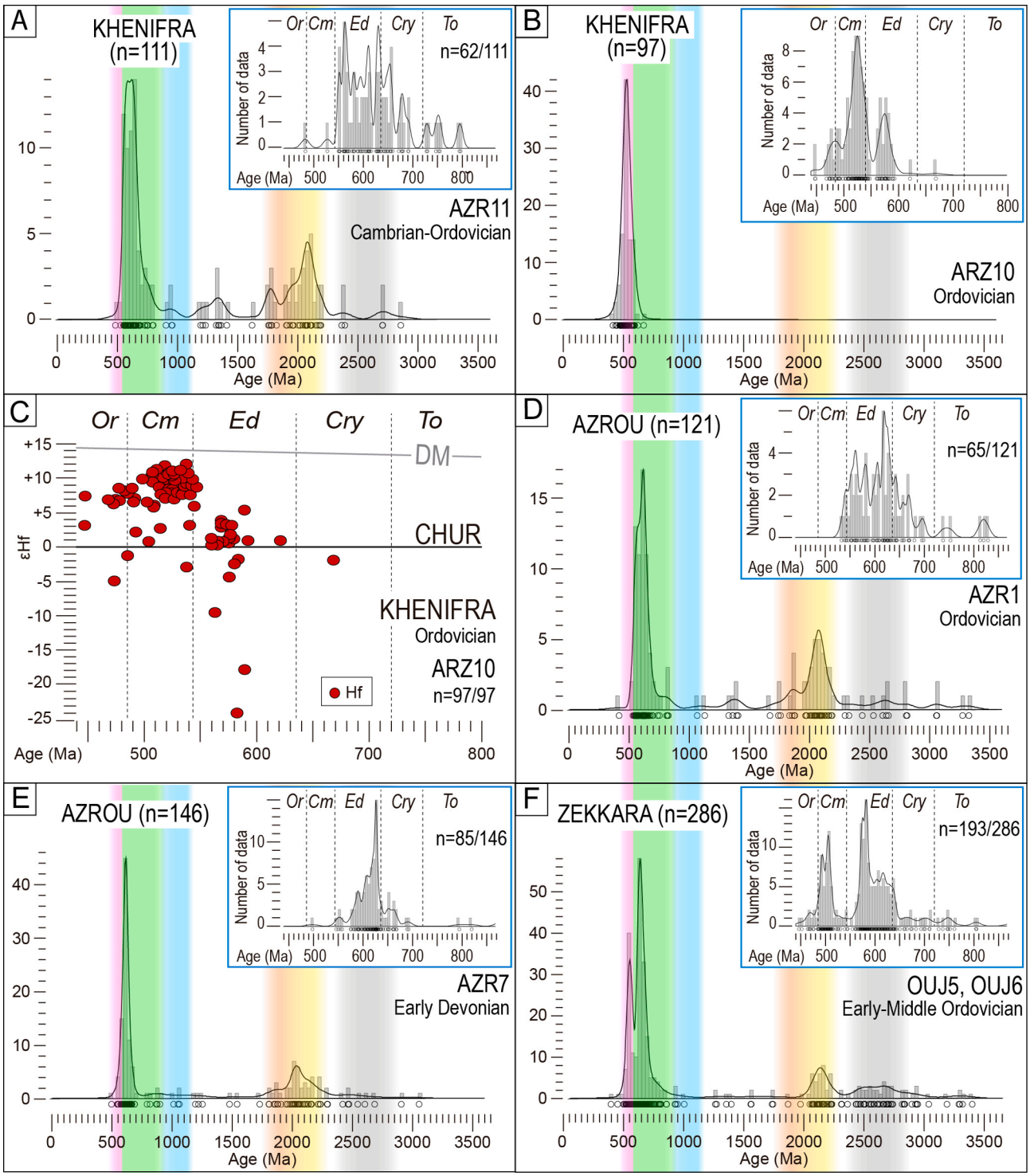

Fig. 4. KDE (black lines) and histograms (grey bars) showing the U–Pb and Hf (red dots) results in the 0–3600 Ma and 440–870 Ma (in the blue boxes) intervals. (A-B) Khenifra area (Nappe Zone, WMM); (C) εHf *versus* age plot in the Khenifra area [CHUR: Chondritic Uniform Reservoir (Iizuka et al., 2015); DM: depleted mantle (Chauvel et al., 2008)]; Ordvician (D) and Devonian (E) samples from Azrou area (Nappe Zone, WMM); (F) Zekkara area (EMM). Color bars indicate the most common detrital zircon populations recognized in all the samples. Legend as in Fig. 3.

One hundred and thirty–six detrital zircon grains from the Devonian (Razin et al., 2001) sample EZ7 were analyzed using LA–ICPMS (99 grains) and SIMS (37 grains) techniques. These analyses yielded a total of 121 concordant results (Table 2 and Fig. 3D), clustered at the following ages:

- Late Tonian–Ediacaran (*c.* 845–553 Ma, n = 40, 33.1% of the data) with a Cryogenian mean age (660.1 ± 0.6 Ma) and multiple peaks at *c.* 610, 630, 645, 665, 695, 725, and 795 Ma.
- Stenian–Tonian (*c.* 1133–858 Ma, n = 33, 27.3% of the data) with a late Stenian mean age (1017.6 ± 1.0 Ma) and a main peak centered at *c.* 1050 Ma.

- Orosirian–Statherian (*c.* 1925–1740 Ma, n = 15, 12.4% of the data) clustered in two peaks at 1749.2 ± 8.9 Ma and 1901.9 ± 3.0 Ma (main peak).
- Rhyacian–Orosirian (*c.* 2117–1947 Ma, n = 17, 14% of the data) with a late Rhyacian mean age (2067.3 ± 1.8) and a main peak centered at *c.* 1995 Ma.
- Neoarchean (*c.* 2774–2600 Ma, n = 8, 6.6% of the data) with a mean age of 2662.2 ± 2.3 Ma.

Scattered data yielded Cambrian (*c.* 526–451 Ma, n = 2), Calymmian–Stenian (*c.* 1424–1222 Ma, n = 3), Siderian (*c.* 2467–2325 Ma, n = 2), and Mesoarchean (*c.* 2986 Ma, n = 1) ages. The youngest detrital zircon population in this sample includes 4 dates and yielded an Ediacaran age (604.5 ± 1.8 Ma, MSWD = 1.52).

4.4. Oulmes area (Central Zone, WMM)

From the Lower Devonian (Kaiser et al., 2007) sample OU5, 148 detrital zircon grains were separated and 150 analyses were carried out, 135 of which yielded concordant results (Fig. 3E). The main detrital zircon age populations recognized in this sample are as follows:

- Late Tonian–Ediacaran (*c.* 862–552 Ma, n = 74, 54.8% of the data) with an early Ediacaran mean age (627.0 ± 0.3 Ma). This population is characterized by a main peak at *c.* 635 Ma and second order peaks at *c.* 565, 590, 610, 660, and 675 Ma; data between *c.* 862 and *c.* 692 Ma show a more scattered pattern.
- Stenian–Tonian (*c.* 1101–922 Ma, n = 9, 6.7% of the data) with a late Stenian mean age (1006.2 ± 2.1 Ma).
- A few Orosirian–Statherian dates (*c.* 1883–1824 Ma, n = 4, 3% of the data) peaked at 1852.1 ± 5.5 Ma (Late Orosirian).
- Rhyacian–Orosirian dates (*c.* 2198–1984 Ma, n = 25, 18.5% of the data) characterized by a Rhyacian mean age (2107.6 ± 2.0 Ma).

Scattered grains yielded Cambrian (*c.* 510 Ma, n = 1), Statherian–-Stenian (*c.* 1711–1163 Ma, n = 9), Orosirian (*c.* 1922 Ma, n = 1), and Mesoarchean–Rhyacian (*c.* 2810–2236 Ma, n = 12) ages. The youngest detrital zircon population in this sample includes 6 dates that define a Late Ediacaran age (562.9 ± 1.5 Ma, MSWD = 0.75).

4.5. Khenifra area (Nappe Zone, WMM)

From the Cambrian–Ordovician (Verset, 1985) sample (AZR11) collected in this area, only 78 detrital zircon grains could be analyzed with LA–ICPMS, yielding 67 concordant results. Other 47 grains, smaller in size, were analyzed with SIMS, having obtained 44 concordant results (Table 2). Combining all the concordant data (Fig. 4A), the following detrital zircon age populations have been recognized:

- Late Tonian–Ediacaran (*c.* 797–550 Ma, n = 60, 54.1% of the data) with a late Ediacaran mean age (630.9 ± 0.4 Ma). Multiple peaks are distributed along the *c.* 550–690 age interval, and several scattered data are older than *c.* 728 Ma.
- Orosirian–Statherian dates (*c.* 1827–1761 Ma, n = 6, 5.4% of the data) peaked at 1777.5 ± 4.9 Ma (Late Orosirian).
- Rhyacian–Orosirian (*c.* 2199–1907 Ma, n = 26, 23.4% of the data) with a late Rhyacian mean age (2057.2 ± 1.5 Ma).

Scattered data yielded Cambrian–Late Ordovician (*c.* 528–483 Ma, n = 2), late Statherian–late Tonian (*c.* 1624–905 Ma, n = 12, partially clustered at 1358.5 ± 2.6 Ma), and Mesoarchean–late Siderian (*c.* 2864–2371 Ma, n = 5) ages. The youngest detrital zircon population in this sample is Late Ediacaran in age (551.6 ± 1.6 Ma, MSWD = 0.09) and comprises 4 dates.

One hundred and twenty zircon grains from the Ordovician (Verset, 1985) sample (AZR10) were separated and analyzed, yielding 97 concordant U–Pb ages. With the exception of two Silurian–Lower Devonian (*c.* 434–412 Ma) and two Cryogenian–early Ediacaran (*c.* 669–622 Ma) scattered grains, all the data are clustered in a late Cambrian peak (531.5 ± 0.3 Ma; Fig. 4B). More careful observation of the detrital zircon spectrum shows the following age distribution:

- Among the Cambrian–Ordovician dates (*c.* 541–448 Ma, n = 66, 68% of the data), 50 of them are peaked at *c.* 524 Ma, while the other 16 are clustered around *c.* 479 Ma. The ε_{Hf} values associated with these ages are mainly positive and clustered between ε_{Hf} *c.* + 5 and + 11 (Fig. 4C), with only a few sub–CHUR values (down to –5.6).
- The Ediacaran dates (*c.* 593–541 Ma, n = 29, 29.9% of the data) peak at 569.2 ± 0.6 Ma. The corresponding ε_{Hf} values are clustered between *c.* 0 and + 5, with a few negative values (down to *c.* –25).

Excluding two Silurian-Lower Devonian zircon grains (which are considered insignificant for the statistical analysis and the geological interpretation), the youngest detrital zircon population of this sample includes 4 dates that define an Early Ordovician age (472.3 ± 1.6 Ma, MSWD = 0.876).

4.6. Azrou area (Nappe Zone, WMM)

One hundred and thirty detrital zircon grains were separated from Ordovician (Bouabdelli et al., 1989) sample AZR1. One hundred of these grains were analyzed by LA–ICPMS; due to the small size of some of the zircons in this sample, 31 SIMS analyses were additionally performed in the 30 remaining grains. In total, we obtained 121 concordant results (90 LA–ICPMS and 31 SIMS), shown in Fig. 4D. The main detrital zircon age populations are as follows:

- Late Tonian–Ediacaran (*c.* 828–541 Ma, n = 63, 52.1% of the data), with a mean age of 631.3 ± 0.5 Ma (early Ediacaran) and peaks distributed along the *c.* 665–540 Ma interval, as well as scattered dates older than *c.* 680 Ma.
- Orosirian–Statherian (*c.* 1883–1765 Ma, n = 6, 5% of the data), peaked at 1854.1 ± 9.9 Ma (late Orosirian).
- Rhyacian–Orosirian (*c.* 2195–1973 Ma, n = 28, 23.1% of the data) with an Orosirian mean age (2081.4 ± 2.5 Ma).

Scattered grains yielded Cambrian–Early Devonian (*c.* 538–415 Ma, n = 2), Statherian–Stenian (*c.* 1745–1067 Ma, n = 8, partially clustered around 1371.6 ± 3.2 Ma), and Archean–Siderian (*c.* 3335–2302 Ma, n = 13) ages. The youngest detrital zircon population in this sample is late Ediacaran (542.4 ± 1.8 Ma, MSWD = 1.15) and includes 4 dates.

From the Devonian (Bouabdelli et al., 1989) sample AZR7, we analyzed 153 zircon grains, yielding 168 analyses, 146 of which were concordant (Fig. 4E). These data can be grouped into 3 detrital zircon age populations:

- Cryogenian–Ediacaran (*c.* 692–546 Ma, n = 82, 56.2% of the data) with an Ediacaran mean age (617.6 ± 0.3 Ma). These dates are clustered at *c.* 625 Ma (main peak), 550, 590, 610, and 655 Ma (secondary peaks).
- Orosirian–Statherian (*c.* 1911–1851 Ma, n = 5, 3.4% of the data) peaked at 1877.4 ± 5.6 Ma (Late Orosirian).
- Rhyacian–Orosirian (*c.* 2243–1955 Ma, n = 32, 21.9% of the data) with a mean age of 2086.7 ± 0.7 Ma (Late Rhyacian).

One zircon grain has a Cambrian date (*c.* 497 Ma), while scattered data yielded late Orosirian–late Tonian (*c.* 1814–795 Ma, n = 16) and Mesoarchean–Rhyacian (*c.* 3064–2296 Ma, n = 10) dates. The youngest detrital zircon population is late Ediacaran (554.2 ± 1.5 Ma, MSWD = 1.66, n = 4).

4.7. Zekkara area (EMM)

From the two Cambrian-Ordovician (Horon, 1952) samples collected in the Zekkara area (OUJ5 and OUJ6), 140 and 150 detrital zircon grains were separated, respectively. A total of 295 LA–ICPMS analyses were performed, yielding 287 concordant results (see details in Table 2). The detrital zircon age populations recognized in both samples are statistically identical and have been plotted together (Fig. 4F):

- Cambrian–Ordovician (*c.* 539–446 Ma, n = 59, 20.6% of the data) with a Cambrian mean age (498.7 ± 0.3 Ma), a main peak at *c.* 505 Ma, and second order peaks at *c.* 460 and 495 Ma.
- Late Tonian–Ediacaran (*c.* 805–544 Ma, n = 134, 46.9% of the data) with a mean age of 609.0 ± 0.3 Ma (Ediacaran). Excluding relatively scattered grains younger than *c.* 560 Ma and older than *c.* 644 Ma, most of the dates cluster at *c.* 580 (main peak) and 615 Ma.
- Rhyacian–Late Orosirian (*c.* 2186–2002 Ma, n = 33, 11.5% of the data) with a late Rhyacian mean age (2103.4 ± 2.9 Ma).
- Neaoarchean–Siderian (*c.* 2694–2386 Ma, n = 27, 9.4% of the data) with a late Siderian mean age (2552.9 ± 2.8 Ma).

Scattered grains yielded Orosirian–Tonian (*c.* 1923–875 Ma, n = 14), early Siderian–Rhyacian (*c.* 2315–2263 Ma, n = 3), and Archean (*c.* 3357–2771 Ma, n = 14) dates. One Early Carboniferous (c. 341 Ma) and one Early Devonian (c. 398 Ma) grains were found in samples OUJ5 and OUJ6, respectively. Nevertheless, they are not statistically significant and, hence, were not taken into account. The youngest detrital zircon population of the two combined samples includes 4 dates that define an Middle Ordovician age (468.7 ± 1.6 Ma, MSWD = 0.38) and postdates the previous stratigraphic age assignement (Cambrian-Ordovician; Horon, 1952). However, when taken separately, the two samples yield late Cambrian-Early Ordovician youngest detrital zircon population ages (470.6 ± 1.6 Ma for sample OUJ5 and 491.0 ± 1.1 Ma for OUJ6).

To sum up, with the exception of the peculiar results obtained in sample AZR10, the late Tonian–Ediacaran and Rhyacian–Orosirian populations are always dominant in the studied samples, representing 33–56% and 11–23% of the data, respectively. The occurrence of minor detrital zircon populations (Neoarchean–Siderian, Orosirian–Statherian, Tonian–Stenian, and Cambrian–Ordovician) is very variable in time and space (Table 3).

5. Discussion

5.1. Maximum depositional ages

The analysis of detrital zircon ages in metasedimentary rocks is a powerful tool to ascertain the possible sources of sediments and constrain maximum age of deposition (MAD; *e.g.*, Fedo et al., 2003). As previously stated, in this work MAD is defined by the youngest detrital zircon population made up of at least 4 dates in each sample or group of statistically homogeneous samples. Thus, the MAD might be virtually coeval or, more commonly, older (up to hundreds of millions of years; Sharman and Malkowski, 2020) than true age of deposition (TAD) inferred from fossil content and/or geochronological dating of volcanic intercalations. The delay between MAD and TAD depends on the geographical and geological setting in which the sedimentary rocks were deposited, such as topography, drainage systems, basin configuration, and tectonic setting (*e.g.*, Sharman and Malkowski, 2020). In those cases in which TAD are poorly constrained, MAD might be taken as a rough approximation of the true depositional age of a sedimentary rock.

In the case of all the Cambrian–Lower Devonian samples studied in this work, TAD (constrained by the biostratigraphic knowledge of the sampled sections) are younger than MAD (Table 3). In most samples, the difference between MAD and TAD is between *c.* 100 and 200 Ma, which supports sedimentation in a passive continental margin free from the influence of magmatic activity (Sharman and Malkowski, 2020).

Table 3
Summary of the detrital zircon populations recognized in the studied samples with approximate ages and percentage of occurrences.

	COASTAL BLOCK	OUED AKREUCH	EZZHILIGA		OULMES	KHENIFRA		AZROU		ZEKKARA
	ORDOVICIAN	*ORDOVICIAN*	*ORDOVICIAN*	*DEVONIAN*	*DEVONIAN*	*ORDOVICIAN*	*CAMBRIAN-ORDOVICIAN*	*ORDOVICIAN*	*DEVONIAN*	*ORDOVICIAN*
YOUNGEST DETRITAL ZIRCON POPULATION	505.8±0.9 Ma MSWD = 0.95 n = 28	549.6±2.1 Ma MSWD = 0.59 n = 5	534.4±1.9 Ma MSWD = 0.43 n = 9	604.5±1.8 Ma MSWD = 1.52 n = 4	562.9±1.5 Ma MSWD = 0.75 n = 6	472.3±1.6 Ma MSWD = 0.86 n = 4	551.6±1.6 Ma MSWD = 0.09 n = 4	542.4±1.8 Ma MSWD = 1.15 n = 4	554.2±1.5 Ma MSWD = 1.66 n = 4	468.7±1.6 Ma MSWD = 0.38 n = 4
CAMBRIAN-ORDOVICIAN *c.* 540-450 Ma	*c.* 507 Ma 36.7%	-	*c.* 520 Ma 2.7%	-	-	*c.* 479 Ma *c.* 524 Ma 68%	-	-	-	*c.* 499 Ma 20.6%
LATE TONIAN-EDIACARAN *c.* 850-540 Ma	*c.* 596 Ma 45.9%	*c.* 639 Ma 49.2%	*c.* 627 Ma 56.1%	*c.* 660 Ma 33.1%	*c.* 627 Ma 54.8%	*c.* 569 Ma 29.9%	*c.* 631 Ma 54.1%	*c.* 631 Ma 52.1%	*c.* 617 Ma56.2%	*c.* 609 Ma 46.9%
STENIAN-EARLY TONIAN *c.* 1080-850 Ma	-	*c.* 974 Ma 8.7%	*c.* 992 Ma 1.9%	*c.* 1015 Ma 26.4%	*c.* 1006 Ma 6.7%	-	-	-	-	-
OROSIRIAN-STATHERIAN *c.* 1950-1750 Ma	-	*c.* 1836 Ma 7.5%	*c.* 1816 Ma 3.5%	*c.* 1749 Ma *c.* 1901 Ma 12.4%	*c.* 1852 Ma 3.0%	-	*c.* 1777 Ma 5.4%	*c.* 1854 Ma 5.0%	*c.* 1877 Ma 3.4%	-
RHYACIAN-OROSIRIAN *c.* 2220-1950 Ma	*c.* 2049 Ma 11.0%	*c.* 2018 Ma *c.* 2143 Ma 20.8%	*c.* 2069 Ma 25.3%	*c.* 2067 Ma 14.0%	*c.* 2108 Ma 18.5%	-	*c.* 2057 Ma 23.4%	*c.* 2081 Ma 23.1%	*c.* 2087 Ma 21.9%	*c.* 2103 Ma 11.5%
NEOARCHEAN -SIDERIAN *c.* 2800-2300 Ma	-	*c.* 2516 Ma 4.7%	*c.* 2412 Ma 4.6%	*c.* 2662 Ma 6.6%	-	-	-	-	-	*c.* 2467 Ma *c.* 2635 Ma 9.4%

Nevertheless, in a few cases, the delay between MAD and TAD is reduced to just a few tens of millions of years (*e.g.*, sample MAN1, Coastal Block) or even less (sample AZR10, Khenifra area, and samples OUJ5 and OUJ6, Zekkara area), suggesting some magmatic activity in the region at Cambrian–Ordovician time, although its relevance, as discussed in section 5.4.1, was probably minor and local.

5.2. Main sediment source: West African Craton affinity

Provenance studies supported by statistical analysis of detrital zircon age distribution are based on the comparison among age spectra of detrital samples and those of potential source areas (*e.g.*, Fedo et al., 2003, and references therein). In the case of the Moroccan Variscides, the typical age spectrum of the West African Craton (WAC; Fig. 5) accords quite well with the patterns found in Ediacaran to Carboniferous metasedimentary rocks (*e.g.*, Abati et al., 2010; Accotto et al., 2019; Accotto et al., 2020; Accotto et al., 2021; Accotto et al., in press; Avigad et al., 2012; El Houicha et al., 2018; Ghienne et al., 2018; Letsch et al., 2018). This source area (WAC) is characterized by late Tonian–Ediacaran (*c.* 750–540 Ma) and Rhyacian–Orosirian (*c.* 2.2–1.95 Ga) ages (Fig. 5), which are related to the Cadomian/Pan–African and Eburnean orogenies, respectively (Nance et al., 2008, and references therein). Furthermore, Neoarchean–Paleoproterozoic ages (*c.* 2.5 Ga) are also common in the WAC and have been generally associated with the Leonian–Liberian orogenies (Hurley et al., 1971; Nance et al., 2008, and references therein). On the contrary, Mesoproterozoic magmatic sources are common in Baltica, Laurentia, Avalonia, Amazonia and other Grenvillian terranes (Ernst et al., 2008), but absent in the WAC and the Tuareg Shield.

Fig. 6 shows a comparison between all the detrital zircon age spectra from lower Cambrian–Lower Devonian detrital metasedimentary rocks described in this work and in previous studies carried out in the Moroccan Mesetas (Accotto et al., 2019; Accotto et al., in press; Ghienne et al., 2018; Letsch et al., 2018). This comparison clearly demonstrates that the main detrital zircon populations in all of the samples are consistent with those that characterize the WAC, supporting a WAC affinity for the studied rocks. The general lack of Mesoproterozoic detrital zircon grains can also be taken as evidence of WAC and/or Tuareg Shield provenance. Furthermore, our new data are also consistent with the detrital zircon spectra from other Neoproterozoic–Lower Paleozoic rocks from the High Atlas and Anti–Atlas (Abati et al., 2010; Avigad et al., 2012; Perez et al., 2019), unanimously supporting the common interpretation that the WAC was the main source region for the sediments deposited in this part of the northern passive margin of Gondwana.

The (meta)igneous rocks that constitute the Precambrian basement of the Moroccan Mesetas (Fig. 1) could have also been the source of detrital zircon grains found in the overlying Paleozoic sedimentary succession. Though very small and scarce, some outcrops have revealed the existence of Eburnean (Pereira et al., 2015) and Cadomian (El Haibi et al., 2020; El Haïbi et al., 2021; El Houicha et al., 2018; Letsch et al., 2018; Ouabid et al., 2017; Tahiri et al., 2010) basement in the Western Meseta. This basement might have been exposed and prone to erosion during the earliest Paleozoic rifting, prior to be covered by the passive

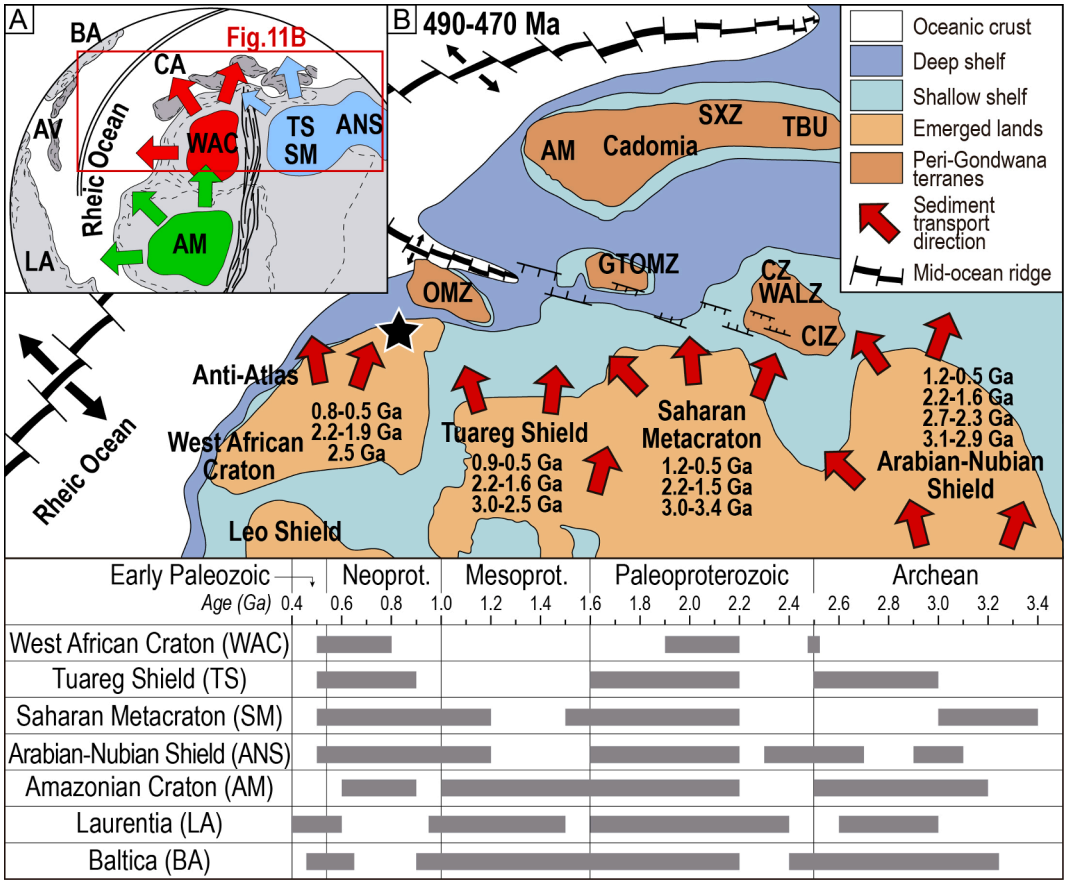

Fig. 5. (A) Paleogeographic reconstruction of the northwestern margin of Gondwana and peri–Gondwanan terranes at Late Ordovician time (490–470 Ma); AM: Amazonia AV: Avalonia; BA: Baltica; CA: Cadomia; LA: Laurussia; TS–SM: Tuareg Shield and Saharan Metacraton; WAC: West African Craton; (B) A more detailed reconstruction with the different cratonic areas. The numbers in the map and the grey bars in the graphical time scale indicate the magmatic zircon age distribution in the main source areas. The studied area is located with a black star. AM: Armorican Massif; CIZ: Central Iberian Zone; CZ: Cantabrian Zone; GTOMZ: Galicia–-Tras–os–Montes Zone; OMZ: Ossa Morena Zone; SXZ: Saxo–Thuringian Zone; TBU: Tepla–Barrandian Unit; WALZ: Western Asturian–Leonese Zone. Modified from Díez Fernández et al. (2010) and Cambeses et al. (2017), and references therein.

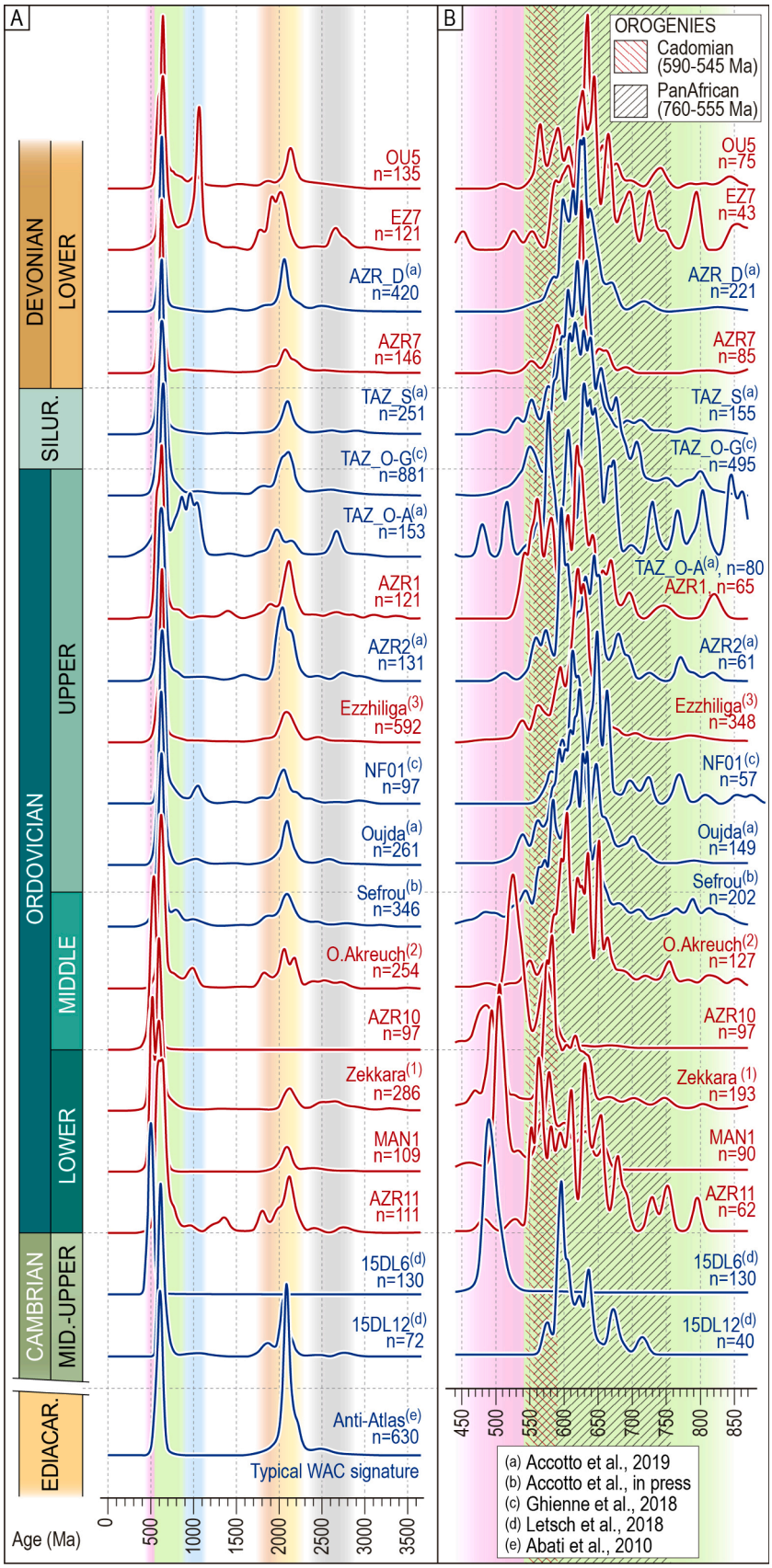

Fig. 6. Comparison among KDE plots from the Moroccan Mesetas; A) entire age spectra (3600–0 Ma); B) Late Tonian–early Silurian spectra (870–440 Ma). Red lines represent samples from this study; blue lines are data from previous works (see references in the Figure); the Ediacaran KDE plot from Anti-Atlas (see reference in the Figure) represents the typical signature of the WAC as reference for the comparison. (1) Zekkara: OUJ5 and OUJ6; (2) Oued Akreuch: AKR1 and AKR2; (3) Ezzhiliga: EZ1, EZ2, EZ4, EZ5, and EZ6.

margin sediments. In particular, two metarhyolites from the Khenifra area yielded protholith ages of *c.* 564 Ma and *c.* 570 Ma (Letsch et al., 2018), in agreement with the *c.* 570 Ma detrital zircon population found in the nearby Cambrian–Ordovician samples AZR10 and AZR11 reported here (Fig. 4A and B).

5.3. Discriminating between Pan–African and Cadomian sources

The late Tonian–Ediacaran detrital zircon population is related to both the Cadomian (590–545 Ma; Linnemann et al., 2008, and references therein) and Pan–African (760–555 Ma; Hefferan et al., 2014, and references therein) orogenies, which partially overlap in time and space. The Pan–African orogeny is commonly considered responsible for the subduction– and collision–related tectonic events that assembled northern Africa during the Neoproterozoic, while the Cadomian orogeny refers to the Andean–type tectonic setting that was active along the northern Gondwana margin during Ediacaran time. In the detailed KDE plots shown in Fig. 6B, it can be observed that the highest peaks of the Late Tonian–Ediacaran population (green background) in the Lower Ordovician samples (AZR11, MAN1, OUJ5 and OUJ6, and AZR10) appear at *c.* 590 and *c.* 555 Ma, *i.e.*, the period of time when the two orogenies overlapped. In contrast, in the Middle Ordovician–Lower Devonian samples, despite the presence of second– and/or third–order peaks at 590–555 Ma, the highest peaks are slightly older (*c.* 650–600 Ma). Accordingly, we suggest that during the early Paleozoic (Cambrian to Early Ordovician), the Moroccan Meseta sediments were sourced from both Cadomian and Pan–African rocks, *i.e.*, from the neighboring and recently active subduction–related continental margin. Later, from Middle Ordovician time onwards, continued subsidence at the continental now passive margin led to the burial of the remaining Cadomian magmatic arc, displacing the main sediment source to inland and more stable areas of the WAC, where Pan–African older rocks cropped out.

5.4. Minor detrital zircon populations and secondary sediment sources

5.4.1. Cambrian–Ordovician magmatism

Despite the predominance of Paleozoic sediments with WAC affinity in the Moroccan Mesetas, the occurrence of minor detrital zircon populations suggests the influence of additional secondary incomes from other terranes and/or local magmatic sources.

In this regard, the presence and distribution of a Cambrian–Ordovician (*c.* 525–480 Ma) detrital zircon population in the Moroccan Mesetas deserves some consideration. All of the available tectonic reconstructions consider that a Cambrian–Ordovician rifting episode followed the cessation of the Cadomian subduction, giving way to a new Wilson cycle during which the Rheic Ocean developed (Fig. 5; *e.g.*, Cambeses et al., 2017; Nance et al., 2012; Nance et al., 2010). This rifting episode is well recognized in the Variscan massifs of central and southern Europe, where it is characterized by thick Cambrian–Ordovician sedimentary successions accompanied by rift–related magmatic rocks (*e.g.*, Álvaro et al., 2018, and references therein; Linnemann et al., 2007, and references therein; Montero et al., 2009; Sánchez–García et al., 2003; Sánchez-García et al., 2019). Detrital zircon grains of Cambrian–Ordovician age are also relatively common in the lower–middle Paleozoic (meta)sedimentary rocks of these regions (*e.g.*, Bahlburg et al., 2010; Drost et al., 2011; Košler et al., 2014; Lin et al., 2019, 2016; Linnemann et al., 2008; Pastor-Galán et al., 2013b; Pereira

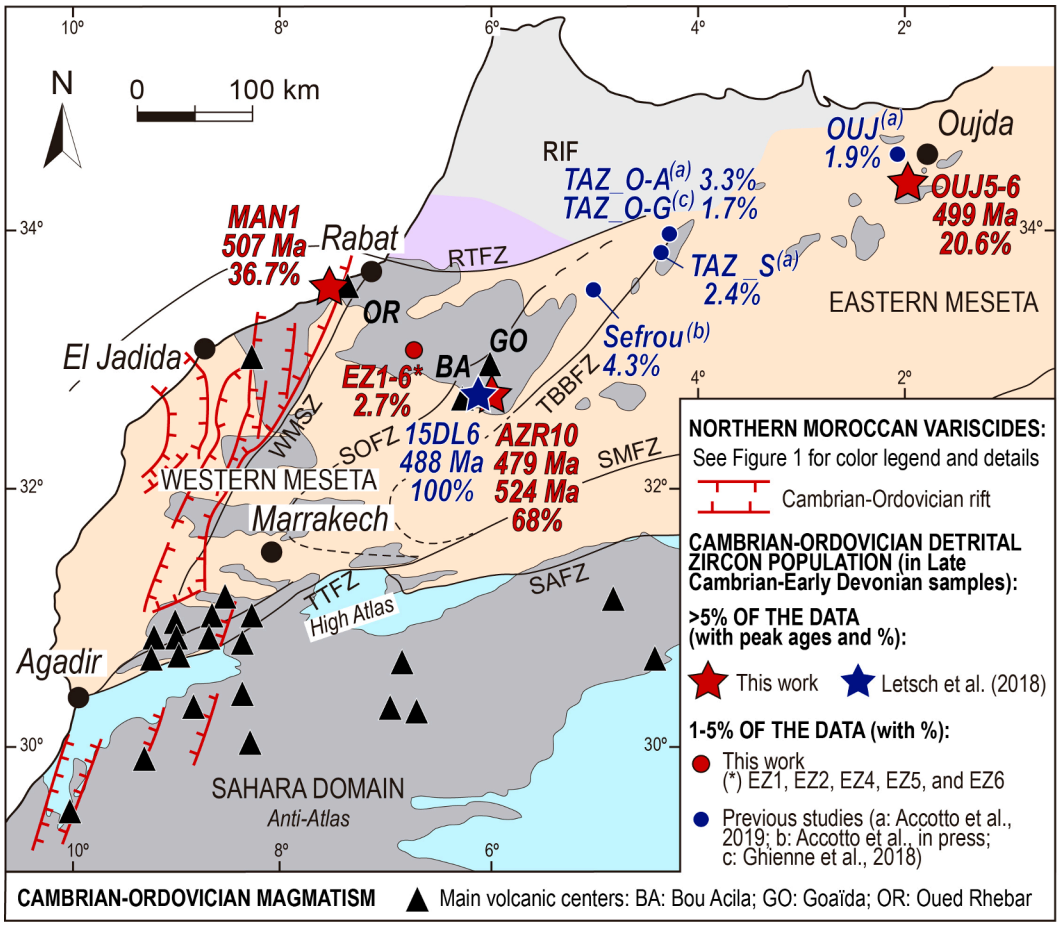

Fig. 7. Distribution of the Cambrian–Ordovician rift and volcanic centers described in northern Morocco (after Pouclet et al., 2018, and references therein; Ouabid et al., 2020), with percentages of the Cambrian–Ordovician detrital zircon populations. See caption of Fig. 1 for acronyms.

et al., 2012; Shaw et al., 2014; Strnad and Mihaljevič, 2005; Szczepański et al., 2020; Talavera et al., 2012; Žák and Sláma, 2018).

In northern Morocco, Cambrian–Ordovician rifting seems to have aborted before reaching the oceanic phase (Bernardin et al., 1988; Ouali et al., 2003; Piqué, 2003; Piqué, 1979; Piqué et al., 1995; Piqué and Michard, 1989). The paleogeographic reconstructions of this rift extend it from the western part of the Anti–Atlas to the northern part of the Coastal Block with a broadly NNE–SSW trend (Fig. 7; *e.g.*, Álvaro et al., 2014; Bernardin et al., 1988; Ezzouhairi et al., 2008; Ouali et al., 2003; Piqué, 2003; Piqué et al., 1995; Piqué and Michard, 1989; Pouclet et al., 2018, and references therein). In the Anti–Atlas, Pouclet et al. (2018, and references therein) recognized 6 magmatic pulses related to the aborted rift, the youngest of which (*c.* 500–497 Ma) also affected the Western Moroccan Meseta in the northern part of the Coastal Block (El Hadi et al., 2006a) and the southern part of the Central Zone (Khenifra area; Fig. 7; Ouabid et al., 2020; Ouali et al., 2003). Nevertheless, Cambrian–Ordovician detrital zircon grains are not common in the Cambrian–Devonian rocks of the Moroccan Mesetas, where they have been only reported locally and, except for an isolated case in the Khenifra area (sample 15DL6 by Letsch et al., 2018), in limited percentages (less than 5% of the data; Fig. 7; Accotto et al., 2019, Accotto et al., in press; Ghienne et al., 2018).

In the new data reported here, the Cambrian–Ordovician detrital zircon population is generally scarce, except in a few Lower–Middle Ordovician samples from the Coastal Block (MAN1), Khenifra (AZR10), and Zekkara (OUJ5 and OUJ6) areas (Fig. 7). In the first two cases, the samples were collected *c.* 10–15 km from the Oued Rhebar and Bou Acila volcanic centers (Pouclet et al., 2018, and references therein), respectively. In the Oued Rhebar sector, acid to intermediate trachyandesites (El Hadi et al., 2006b) yielded a geochronological age of 507 ± 5 Ma (U–Pb on magmatic zircon grains; El Attari et al., 2019), perfectly coincident with the average age of the Cambrian peak found in MAN1 (*c.* 507 Ma, 36.7% of the data). In the Bou Acila sector, at least two magmatic events imprecisely dated, but separated by lower Cambrian limestones, were recognized (Morin, 1960; Ouali et al., 2003; Pouclet et al., 2018; Verset, 1988). Interestingly, Letsch et al. (2018) published data from a sample of this sector (15DL6, Figs. 6 and 7), which depicts a single late Cambrian (*c.* 488 Ma) detrital zircon peak; this sample suggests that at least one magmatic pulse in the Bou Acila sector occurred at late Cambrian time. Furthermore, detrital zircon ages from nearby sample AZR10 show a main peak at *c.* 524 Ma (52% of the data) and a minor one at *c.* 479 Ma (16% of the data) (Fig. 6B), both characterized by positive ε_{Hf} values clustered between +5 and +11 (Fig. 4C). These peaks can be tentatively related to other magmatic pulses of the Bou Acila volcanic center. The positive ε_{Hf} values seem to confirm the juvenile nature of some of the magmas associated with the rifting episode.

In both the Coastal Block and Khenifra samples, however, the overall imprint of Cambrian magmatism might have been limited, since almost coeval samples collected *c.* 40 km away from the Oued Rhebar (AKR1 and AKR2, Lower–Upper Ordovician) and Bou Acila (AZR11, Cambrian–Ordovician) volcanic centers, as well as a slightly younger sample located very close to the Oued Rhebar sector (NF01, Upper Ordovician, Ben Slimane area; Ghienne et al., 2018) contain only a couple of scattered Cambrian grains or none at all (Fig. 6B).

In the Eastern Moroccan Meseta, no Cambrian–Ordovician volcanic centers have been reported until now, but the samples from Zekkara (OUJ5 and OUJ6, Fig. 1D, 1B and 7) yielded 20.6% of Cambrian–Ordovician ages (mean age *c.* 499 Ma), suggesting that at least one magmatic source of that age existed in that area. Nevertheless, other Late Ordovician samples from the nearby Oujda area (15 km NE from Zekkara) only yielded 1.9% of Cambrian ages (Accotto et al., 2019), which points to a very local influence of any Cambrian–Ordovician EMM magmatic source.

The occurrence of Cambrian–Ordovician detrital zircon grains sensibly decreases in Middle Ordovician–Silurian samples (≤5% of the data), while in the Lower Devonian ones almost no Cambrian–Ordovician detrital zircon ages have been found (Fig. 6B). These data suggest, therefore, that shortly after rift abortion (Bernardin et al., 1988; Ouali et al., 2003; Piqué, 2003; Piqué, 1979; Piqué et al., 1995; Piqué and Michard, 1989) and a brief erosional phase, the volcanic centers in the Moroccan Meseta were probably covered by the passive margin sedimentary sequence, mainly fed by erosion of the WAC and partial recycling of older sedimentary rocks.

5.4.2. *Stenian–early Tonian detrital zircon ages*

Another minor detrital zircon population already discussed by several authors in the northern Moroccan Variscides is the Stenian–early Tonian one (*c.* 1.0 Ga). This population was described in middle Cambrian rocks from the Anti–Atlas (Avigad et al., 2012), a Lower Ordovician rock from the Coastal Block (WMM; sample NF01; Fig. 6A; Ghienne et al., 2018), Lower–Middle Ordovician and Upper Ordovician–Silurian rocks from the Middle Atlas (WMM; Fig. 6A; Accotto et al., 2019, Accotto et al., in press; Ghienne et al., 2018), Upper Devonian rocks from the Central Zone (WMM; Accotto et al., 2021), and Upper Ordovician (Fig. 6A), middle–upper Carboniferous rocks from the EMM (Oujda and Jerada areas; Accotto et al., 2019; Accotto et al., 2021). Among the samples analyzed in this study, we have identified the *c.* 1 Ga detrital zircon population in two Middle Ordovician rocks from the Oued Akreuch area (AKR1 and AKR2, 8.7% of the data), five Ordovician (EZ1, EZ2, EZ4, EZ5, and EZ6, 1.9%) and two Lower Devonian rocks from the Ezzhiliga (EZ7, 26.4%) and Oulmes (OU5, 6.7%) areas. In the remaining samples, Mesoproterozoic ages are absent or represented by scarce and scattered grains that cannot be considered as a proper detrital zircon age population (Table 3).

Stenian–early Tonian sources are virtually unknown in the WAC and Tuareg Shield, although recent work (El Bouougri et al., 2020) pointed out the existence of limited early Tonian (*c.* 883 Ma) magmatic activity in the Anti–Atlas related to an incipient phase of Rodinia breakup. Nevertheless, even if this event was sufficiently widespread to provide zircon grains to the Moroccan Mesetas, it could only explain the youngest dates within the Stenian–early Tonian detrital zircon population found in our samples.

Ages ranging from *c.* 1.3 to *c.* 0.9 Ga are typical of the Grenvillian terranes (Ernst et al., 2008) that, before the opening of the Rheic Ocean at Cambrian–Ordovician time (Nance et al., 2012; Nance et al., 2010), were relatively close to the northern Gondwanan margin (*e.g.*, Amazonia). Nevertheless, these terranes are also characterized by other Mesoproterozoic sources in the range 1.7–1.1 Ga (Fig. 5). Interestingly, detrital zircon age distributions compatible with Amazonian sources were found in Neoproterozoic metasedimentary rocks overlying the western WAC in Mauritania (Fig. 1A; Bradley et al., 2015). In contrast, all of the Neoproterozoic–Carboniferous metasedimentary rocks sampled from the Anti–Atlas (*e.g.*, Abati et al., 2010; Avigad et al., 2012) and further north in the High Atlas (Perez et al., 2019) and Moroccan Mesetas (Accotto et al., 2019; Accotto et al., 2021, Accotto et al.,in press; El Houicha et al., 2018; Ghienne et al., 2018; Letsch et al., 2018; this work), did not record Mesoproterozoic ages older than *c.* 1.1 Ga (except for a very few scattered grains, *e.g.*, AZR11 and AZR1; Fig. 6A). Therefore, it is very unlikely that Amazonian (*c.* 1.7–0.9 Ga) sources could have supplied the *c.* 1.0 Ga detrital zircon population, episodically found in the northern Moroccan Variscides. As an exception, a statistically significant number of detrital zircon grains yielded dates between *c.* 1.7 and 1.1 Ga in a few lower Carboniferous samples from the Mohammedia (Coastal Block), Tiflet (northern Central Zone), and Debdou–Mekkam (EMM) areas (Fig. 1; Accotto et al., 2020, Accotto et al., 2021). In these specific cases, the authors invoked an Avalonian (Amazonia–derived) source only available since the early Variscan (Tournaisian–early Visean) collision.

To explain the occurrences of *c.* 1.0 Ga detrital zircon ages in the pre–collisional succession of the northern Moroccan Variscides, several authors (Accotto et al., 2019; Accotto et al., 2021; Accotto et al., in press

i; Avigad et al., 2012; Ghienne et al., 2018) suggested northeastern African sources (*e.g.*, Saharan Metacraton, Arabian–Nubian Shield; Fig. 5). These sources were first called to explain the presence of Stenian–early Tonian detrital zircon populations in Ordovician–Devonian samples from Lybia (Meinhold et al., 2011). The age spectra of our samples containing the *c.* 1.0 Ga detrital zircon population are compatible with such a northeastern African sources (Fig. 6A).

The spatial and temporal distribution of samples containing Stenian–early Tonian dates is highly irregular, and the statistical relevance of this population is also variable (Fig. 6A). In most cases, grains of this age represent less than 10% of the data, but can locally reach *c.* 25% (*e.g.*, sample EZ7 from this work and the Ordovician samples from the Tazekka area in Accotto et al., 2019). This irregularity contrasts with other northern Gondwanan terranes cropping out in central and northwestern Iberia, where the *c.* 1.0 Ga detrital zircon population is very common and represents 30–50% of the data (Bea et al., 2010; Fernández-Suárez et al., 2014; Gutiérrez-Alonso et al., 2015; Pastor-Galán et al., 2013a; Shaw et al., 2014; Talavera et al., 2012). Accordingly, we suggest that at Ordovician–Early Devonian time, the Moroccan Mesetas belonged to the northern Gondwana passive margin, but in a more western and distal position than the current central/northwestern Iberian terranes (Fig. 5), and, hence, the sedimentary influx from northeastern African primary sources was distant and intermittent.

The *c.* 1.0 Ga detrital zircon grains found in northern Morocco might have been fed from intermediate sedimentary repositories such as the lower Paleozoic, North-directed Gondwanan super–fan system proposed by Meinhold et al. (2013). Nevertheless, the high proportion of *c.* 1.0 Ga zircon grains found in some samples (*e.g.*, sample EZ7 from this work and the Ordovician samples from the Tazekka area in Accotto et al., 2019) suggests a rather direct primary source.

5.4.3. Orosirian–Statherian detrital zircon ages

The Orosirian–Statherian (*c.* 1.95–1.75 Ga) detrital zircon population found in NW Africa is considered by several authors to be related to the last pulses of the Eburnean orogeny (*e.g.*, Abati et al., 2012; Bessoles, 1977; Ghienne et al., 2018). Nevertheless, magmatic rocks related to this orogeny show ages not younger than *c.* 1.95 Ga (Rb/Sr, Sm/Nd, and U/Pb methods; Abouchami et al., 1990; Aït Malek et al., 1998; Boher et al., 1992; Hirdes et al., 1992; Liégeois et al., 1991; Schofield et al., 2006). Statherian (*c.* 1.75 Ga) bimodal dykes were described and dated in the Anti–Atlas, and considered to be the only remnants of a large igneous province developed during the breakup of the Nuna/Columbia supercontinent (Gasquet et al., 2004; Lama et al., 1993; Youbi et al., 2013) during the vanishing stages of the Eburnean orogeny. However, it is unlikely that volumetrically small dyke intrusions could have produced the amount of Orosirian–Statherian detrital zircon grains found in our samples (up to 12.4% of the data in sample EZ7; Table 3) and in other Paleozoic samples from the northern Moroccan Variscides (*e.g.*, Abati et al., 2010; Accotto et al., 2019; Accotto et al., 2020; Accotto et al., 2021; Accotto et al., in press; Avigad et al., 2012; Ghienne et al., 2018; Letsch et al., 2018).

Recent U–Pb dating on zircon grains in charnockites from the Mazagan escarpment, offshore the western Moroccan coast, highlighted crystallization ages varying from *c.* 1.95 to *c.* 1.75 Ga (Kuiper, 2019; Kuiper et al., 2019; Kuiper et al., 2021). These ages are compatible with those found in detrital samples from the northern Moroccan Variscides, including those studied in this work. However, the available data on the Mazagan escarpment are still scarce and, even if it is possible that at least part of the Orosirian–Statherian zircon grains were sourced in this terrane, the uncertainty still remains.

Other Orosirian–Statherian sources are known in Amazonia, Laurentia, and Baltica (Fig. 5; Linnemann et al., 2011, and references therein; Nance et al., 2008). However, as previously discussed for the provenance of the Stenian–early Tonian detrital zircon population (see Section 5.4.2), we exclude these terranes as possible sources because they would have provided also zircon grains in the range 1.75–1.2 Ga, which are generally absent in our samples. Alternatively, northeastern African sources (*e.g.*, Tuareg Shield, Saharan Metacraton, Arabian–Nubian Shield; Fig. 5) might have provided both the Stenian–early Tonian and Orosirian–Statherian detrital zircon grains. If this was the case, we would expect a simultaneous occurrence of both detrital zircon age populations, something that does not always occur (Table 3 and Fig. 6A).

To conclude, based on the data available we cannot define a unique source for the Orosirian–Statherian detrital zircon grains found in our samples and other rocks from the northern Moroccan Variscides (*e.g.*, Abati et al., 2010; Accotto et al., 2019; Accotto et al., 2020; Accotto et al., 2021; Accotto et al., in press; Avigad et al., 2012; Ghienne et al., 2018; Letsch et al., 2018). Nonetheless, admitting that both the WAC and northeastern African cratons (*e.g.*, Saharan Metacraton) were the source of sediments on the passive margin of northern Gondwana during the Paleozoic, it is possible that the 1.95–1.75 Ga detrital zircon grains were actually sourced from different areas.

5.5. Relevance of the tectonic boundaries within the Moroccan Mesetas

The Moroccan Mesetas have been historically divided into several domains separated by fault zones (see Section 1, Fig. 1B). The tectonic relevance and significance of these boundaries is still under debate (*e.g.*, Hoepffner et al., 2006; Michard et al., 2010b; Michard et al., 2010a; Simancas et al., 2010; Simancas et al., 2009).

According to some authors (*e.g.*, Hoepffner et al., 2006, and references therein; Michard et al., 2010a, and references therein, Michard et al., 2010b), the faults bounding the different domains in the Moroccan Mesetas accommodated tens to hundreds of kilometers of displacement related to an important E–W oriented Variscan shortening. Nevertheless, the stratigraphic similarities between the Paleozoic successions within the Moroccan Mesetas and the Anti–Atlas (Piqué, 1994) suggest that there was a paleogeographic continuity between these regions. Furthermore, within the Moroccan Mesetas, our data on detrital zircon grains in the Cambrian–Lower Devonian successions from different areas also support this paleogeographic continuity. In particular, if the easternmost parts of the Moroccan Mesetas were located in a more eastern position, as suggested by Michard et al. (2010b, and references therein), we would expect an increase of Stenian–early Tonian detrital zircon ages there. Nevertheless, the presence and distribution of these NE African sources is highly irregular and does not show a systematic eastward increase. Similarly, other minor detrital zircon populations found in samples from diverse areas and with different ages do not seem to be geographically controlled. The internal boundaries within the Moroccan Mesetas, therefore, seem to have had a limited effect on sedimentation in the different domains. Nonetheless, further tectono–metamorphic studies are needed to better constrain the tectonic relevance of the intra–Mesetas fault zones.

6. Conclusions

New U–Pb geochronological data on detrital zircon grains from 16 Cambrian–Lower Devonian samples from different zones of the Moroccan Mesetas show homogeneous age–frequency distributions. This similarity points to paleogeographical irrelevance of the proposed tectonic boundaries between the different zones/domains (with the exception of the Caledonian Sehoul Block) usually considered in the Moroccan Variscides, in accordance with other geological evidence (comparable stratigraphic successions, absence of ophiolite and/or high–pressure metamorphic belts). The main detrital zircon populations common to our samples have late Tonian–Ediacaran (*c.* 850–540 Ma) and Rhyacian–Orosirian ages (*c.* 2220–1950 Ma), which suggest that the West African Craton was the main source of sediments for this part of the northern Gondwanan margin at early–middle Paleozoic time. Particularly, the Cadomian orogen (*c.* 590–540 Ma) constituted the main source during the Cambrian–Early Ordovician sedimentation, while erosion of

slightly older Pan–African basement (*c.* 650–600 Ma) prevailed from the Middle Ordovician onwards. This change in the main sediment source during the Ordovician can be explained in terms of the progressive dismantling and burial of the Cadomian arc–related rocks at the continental margin, shifting the main source region to older areas located inland of the West African Craton.

The presence of additional minor detrital zircon populations suggests sediment income from other secondary sources such as Cambrian–Lower Ordovician rift-related local volcanic centers and northeastern African basement (*e.g.*, Saharan Metacraton and Arabian–Nubian Shield).

7. Data availability

Supporting data related to this work include cathodoluminescence images (Appendix A), analytical methods (Appendix B), U–Pb data (Appendix C), and Hf data (Appendix D), and they are available at the Mendeley Data repository (doi: 10.17632/vw94rkbx75.1; https://doi.org/10.17632/vw94rkbx75.1)

CRediT authorship contribution statement

Cristina Accotto: Conceptualization, Data curation, Formal analysis, Investigation, Methodology, Software, Visualization, Writing - original draft, Writing - review & editing. **David Martínez Poyatos:** Conceptualization, Funding acquisition, Investigation, Project administration, Supervision, Validation, Writing - original draft, Writing - review & editing. **Antonio Azor:** Conceptualization, Investigation, Supervision, Validation, Writing - original draft, Writing - review & editing. **Cristina Talavera:** Formal analysis, Methodology, Software, Writing - review & editing. **Noreen J. Evans:** Formal analysis, Methodology, Software, Writing - review & editing. **Antonio Jabaloy–Sánchez:** Conceptualization, Investigation, Writing - review & editing. **Abdelfatah Tahiri:** Resources, Writing - review & editing. **Hassan El Hadi:** Resources. **Ali Azdimousa:** Resources.

Declaration of Competing Interest

The authors declare that they have no known competing financial interests or personal relationships that could have appeared to influence the work reported in this paper.

Acknowledgements

This study was found by the Ministerio de Economía y Competitividad (MINECO) of Spain through the project PANGEATOR (CGL2015–71692) and the Pre–Doctoral scholarship BES–2016–078168. We are indebted to Mike Hall and Brad McDonald for their assistance and technical support on sample preparation and the LA–ICPMS, respectively. The CL imaging was carried out on the Curtin University's Microscopy & Microanalysis Facility, whose instrumentation has been partially funded by the University, State and Commonwealth Governments, and the Scanning Electron Microscope (SEM) Facility at the University of Edinburgh. Analysis in the SHRIMP and GeoHistory Facilities, JdLC, Curtin University were enabled by AuScope (auscope.org.au) and the Australian Government via the National Collaborative Research Infrastructure Strategy (NCRIS) and an Australian Geophysical Observing System grant provided to AuScope Pty Ltd. by the AQ44 Australian Education Investment Fund program, respectively. The NPII multi–collector was obtained via funding from the Australian Research Council LIEF program (LE150100013). The SIMS analyses were performed at the NERC Ion Microprobe Facility of the University of Edinburgh (UK). Comments from two anonymous reviewers and editorial handling by Prof. Victoria Pease are acknowledged. Funding for open access charge: Universidad de Granada / CBUA.

Appendix A. Supplementary data

Supplementary data to this article can be found online at https://doi.org/10.1016/j.precamres.2021.106366.

References

Abati, J., Aghzer, A.M., Gerdes, A., Ennih, N., 2012. Insights on the crustal evolution of the West African Craton from Hf isotopes in detrital zircons from the Anti-Atlas belt. Precambrian Res. 212–213, 263–274. https://doi.org/10.1016/j.precamres.2012.06.005.

Abati, J., Mohsine Aghzer, A., Gerdes, A., Ennih, N., 2010. Detrital zircon ages of Neoproterozoic sequences of the Moroccan Anti-Atlas belt. Precambrian Res. 181, 115–128. https://doi.org/10.1016/j.precamres.2010.05.018.

Abouchami, W., Boher, M., Michard, A., Albarede, F., 1990. A major 2.1 Ga event of mafic magmatism in West Africa: an early stage of crustal accretion. J. Geophys. Res. 95, 17605–17629.

Accotto, C., Martínez Poyatos, D., Azor, A., Jabaloy-Sánchez, A., Talavera, C., Evans, N. J., Azdimousa, A., 2020. Tectonic Evolution of the Eastern Moroccan Meseta: From Late Devonian Forearc Sedimentation to Early Carboniferous Collision of an Avalonian Promontory. Tectonics 39, 1–29. https://doi.org/10.1029/2019TC005976.

Accotto, C., Martínez Poyatos, D., Azor, A., Talavera, C., Evans, N.J., Jabaloy-Sánchez, A., Azdimousa, A., Tahiri, A., El Hadi, H., 2021. Syn–collisional detrital zircon source evolution in the northern Moroccan Variscides. Gondwana Res. 93, 73–88. https://doi.org/10.1016/j.gr.2021.02.001.

Accotto, C., Martínez Poyatos, D., Azor, A., Talavera, C., Evans, N.J., Jabaloy–Sánchez, A., El Hadi, H., Tahiri, A. (in press). Detrital zircon sources in the Ordovician metasedimentary rocks of the Moroccan Meseta: inferences for northern Gondwanan passive margin paleogeography. In: Kuiper, Y., Murphy, J.B., Nance, R.D., Strachan, R.A., Thompson, M.D. (Eds.), New developments in the Appalachian–Caledonian–Variscan orogen, GSA books, Special Publication.

Accotto, C., Martínez Poyatos, D.J., Azor, A., Talavera, C., Evans, N.J., Jabaloy-Sánchez, A., Azdimousa, A., Tahiri, A., El Hadi, H., 2019. Mixed and recycled detrital zircons in the Paleozoic rocks of the Eastern Moroccan Meseta: Paleogeographic inferences. Lithos 338–339, 73–86. https://doi.org/10.1016/j.lithos.2019.04.011.

Aït Malek, H., Gasquet, D., Bertrand, J.M., Leterrier, J., 1998. Eburnian and Panafrican granitoids from the Igherm, Kerdous and Bas-Drâa Proterozoic inliers (western Anti-Atlas, Morocco): U-Pb geochronology on zircon. Comptes Rendus l'Académie des Sci. – Ser. IIA – Earth Planet. Sci. 327, 819–826.

Álvaro, J.J., Casas, J.M., Clausen, S., Quesada, C., 2018. Early Palaeozoic geodynamics in NW Gondwana. J. Iber. Geol. 44, 551–565. https://doi.org/10.1007/s41513-018-0079-x.

Álvaro, J.J., Pouclet, A., Ezzouhairi, H., Soulaimani, A., Bouougri, E.H., Imaz, A.G., Fekkak, A., 2014. Early Neoproterozoic rift–related magmatism in the Anti-Atlas margin of the West African craton. Morocco. Precambrian Res. 255, 433–442. https://doi.org/10.1016/j.precamres.2014.10.008.

Arboleya, M.L., Teixell, A., Charroud, M., Julivert, M., 2004. A structural transect through the High and Middle Atlas of Morocco. J. African Earth Sci. 39, 319–327. https://doi.org/10.1016/j.jafrearsci.2004.07.036.

Avigad, D., Gerdes, A., Morag, N., Bechstädt, T., 2012. Coupled U-Pb–Hf of detrital zircons of Cambrian sandstones from Morocco and Sardinia: Implications for provenance and Precambrian crustal evolution of North Africa. Gondwana Res. 21, 690–703. https://doi.org/10.1016/j.gr.2011.06.005.

Bahlburg, H., Vervoort, J.D., DuFrane, S.A., 2010. Plate tectonic significance of Middle Cambrian and Ordovician siliciclastic rocks of the Bavarian Facies, Armorican Terrane Assemblage, Germany – U-Pb and Hf isotope evidence from detrital zircons. Gondwana Res. 17, 223–235. https://doi.org/10.1016/j.gr.2009.11.007.

Baudin, T., Chèvremont, P., Razin, P., Youbi, N., Andries, D., Hoepffner, C., Thiéblemont, D., Chihani, E.M., Tegyey, M., 2003. Carte géologique du Maroc au 1/50.000, feuille 435bis Skhour des Rehamna. Mémoire explicatif. Notes Mem. du Serv. Géologique du Maroc.

Bea, F., Montero, P., Talavera, C., Abu Anbar, M., Scarrow, J.H., Molina, J.F., Moreno, J. A., 2010. The palaeogeographic position of Central Iberia in Gondwana during the Ordovician: Evidence from zircon chronology and Nd isotopes. Terra Nov. 22, 341–346. https://doi.org/10.1111/j.1365-3121.2010.00957.x.

Becker, R.T., El Hassani, A., 2020. Devonian to Lower Carboniferous stratigraphy and facies of the Moroccan Meseta: implications for palaeogeography and structural Interpretation – a project outline. Front. Sci. Eng. 10, 9–25.

Berkhli, M., Vachard, D., Tahiri, A., Paicheler, J.-C., 1999. Stratigrafie séquentielle du Viséen supérieur du bassin de Jerada (Maroc oriental). Eclogae Geol. Helv. 92, 285–294.

Bernardin, C., Cornée, J.J., Corsini, M., Mayol, S., Muller, J., Tayebi, M., 1988. Variations d'épaisseur du Cambrien moyen en Meseta marocaine occidentale: signification géodynamique des données de surface et de subsurface. Can. J. Earth Sci. 25, 2104–2117.

Bessoles, B., 1977. Le Craton Ouest Africain. Geologie de l'Afrique. Mémoires du Bur. Rech. Géologiques Minières 88, 404.

Bhija, F., Fedan, B., Laadila, M., 1999. Les turbidites calcaires siluro–lochkoviennes de la zone de Rabat-Tiflet (Meseta nord–occidentale, Maroc): analyse sédimentologique et implications paléogéographiques. Géologie Méditerranéenne 26, 245–257. https://doi.org/10.3406/geolm.1999.1660.

Boher, M., Abouchami, W., Michard, A., Albarede, F., Arndt, N.T., 1992. Crustal growth in West Africa at 2.1 Ga. J. Geophys. Res. 97, 345–369. https://doi.org/10.1029/91JB01640.
Bouabdelli, M., 1982. Stratigraphie et évolution structurale du Paléozoïque d'Azrou. Université Louis Pasteur, Strasbourg.
Bouabdelli, M., Cailleux, Y., Hoepffner, C., Michard, A., Pique, A., 1989. Le bassin dinantien d'Azrou et l'évolution de sa déformation hercynienne (Méséta marocaine nord–ordientale). Notes Mem. du Serv. Géologique du Maroc 335, 221–227.
Bouabdelli, M., Piqué, A., 1996. Du bassin sur décrochement au bassin d'avant–pays: dynamique du bassin d'Azrou–Khénifra (Maroc hercynien central). J. Africa 23, 213–224.
Bradley, D.C., O'Sullivan, P., Cosca, M.A., Motts, H.A., Horton, J.D., Taylor, C.D., Beaudoin, G., Lee, G.K., Ramezani, J., Bradley, D.B., Jones, J.V., Bowring, S.A., 2015. Second projet de renforcement institutionnel du secteur minier de la République Islamique de Mauritanie (PRISM–II). Synthesis of geological, structural, and geochronologic data: Phase V, Deliverable 53. https://doi.org/10.3133/ofr20131280.
Braid, J.A., Murphy, J.B., Quesada, C., Mortensen, J., 2011. Tectonic escape of a crustal fragment during the closure of the Rheic Ocean: U-Pb detrital zircon data from the Late Palaeozoic Pulo do Lobo and South Portuguese zones, southern Iberia. J. Geol. Soc. London. 168, 383–392. https://doi.org/10.1144/0016-76492010-104.
Cailleux, Y., 1994. Introduction historique et structurale. (Le Massif central marocain et la Meseta oriental). Bull. l'Institut Sci. Rabat 18, 10–31.
Cambeses, A., Scarrow, J.H., Montero, P., Lázaro, C., Bea, F., 2017. Palaeogeography and crustal evolution of the Ossa-Morena Zone, southwest Iberia, and the North Gondwana margin during the Cambro–Ordovician: a review of isotopic evidence. Int. Geol. Rev. 59, 94–130. https://doi.org/10.1080/00206814.2016.1219279.
Charriere, A., 1990. Héritage hercynien et évolution géodynamique alpine d'une chaîne intracontinentale: le Moyen-Atlas au SE de Fes (Maroc). Ph.D. Thesis. Université de Toulouse 3, France.
Charriere, A., 1989. Carte géologique du Maroc No354: Sefrou – Echelle 1/100.000. Roy. du Maroc, Ministère l'Energie des Mines du Développement Durable.
Chauvel, C., Lewin, E., Carpentier, M., Arndt, N.T., Marini, J.-C., 2008. Role of recycled oceanic basalt and sediment in generating the Hf–Nd mantle array. Nat. Geosci. 1, 64–67. https://doi.org/10.1038/ngeo.2007.51.
Choubert, G., Marçais, J., Suter, G., 1978. Carte géologique du Maroc – 1/500.000: Oujda. Roy. du Maroc, Ministère l'Energie des Mines du Développement Durable.
Desteucq, C., Fournier-Vinas, C., 1981. Présence d'Ordovicien dans la règion d'Oujda. Mines, Géologie Energ, p. 50.
Destombe, J., 1987. Carte géologique du Maroc No350: Casablanca–Mohammedia – Echelle 1/100.000. Roy. du Maroc, Ministère l'Energie des Mines du Développement Durable.
Destombe, J., Jeannette, A., 1966. Mémoire explicatif de la carte géotechnique de la Meseta côtère à l'Est de Casablanca. Régions de Mohammedia, Bouznika et Ben Slimane. Notes Mem. du Serv. Géologique du Maroc 180, 104.
Dickinson, W.R., Gehrels, G.E., 2009. Use of U-Pb ages of detrital zircons to infer maximum depositional ages of strata: A test against a Colorado Plateau Mesozoic database. Earth Planet. Sci. Lett. 288, 115–125. https://doi.org/10.1016/j.epsl.2009.09.013.
Díez Fernández, R., Catalán, J.R.M., Gerdes, A., Abati, J., Arenas, R., Fernández-Suárez, J., 2010. U-Pb ages of detrital zircons from the Basal allochthonous units of NW Iberia: Provenance and paleoposition on the northern margin of Gondwana during the Neoproterozoic and Paleozoic. Gondwana Res. 18, 385–399. https://doi.org/10.1016/j.gr.2009.12.006.
Drost, K., Gerdes, A., Jeffries, T., Linnemann, U., Storey, C., 2011. Provenance of Neoproterozoic and early Paleozoic siliciclastic rocks of the Teplá-Barrandian unit (Bohemian Massif): Evidence from U-Pb detrital zircon ages. Gondwana Res. 19, 213–231. https://doi.org/10.1016/j.gr.2010.05.003.
Eckelmann, K., Nesbor, H.–D., Königshof, P., Linnemann, U., Hofmann, M., Lange, J.–M., Sagawe, A., 2014. Plate interactions of Laurussia and Gondwana during the formation of Pangaea – Constraints from U–Pb LA–SF–ICP–MS detrital zircon ages of Devonian and Early Carboniferous siliciclastics of the Rhenohercynian zone, Central European Variscides. Gondwana Res. 25, 1484–1500. doi:10.1016/j.gr.2013.05.018.
El Attari, A., Pereira, M.F., Ezzouhairi, H., El Houicha, M., Jouhari, A., Berrada, I., Fekkak, A., Ennih, N., Hoepffner, C.H., Gama, C., Silva, J.B., 2019. Zircon U-Pb geochronology and geochemistry of Cambrian magmatism in the Coastal Block (Oued Rhebar volcanic complex, Moroccan Meseta): Implications for the geodynamic evolutionary model of North-Gondwana. J. African Earth Sci. 160, 103598 https://doi.org/10.1016/j.jafrearsci.2019.103598.
El Bouougri, H., Lahna, A.A., Tassinari, C.C.G., Basei, M.A.S., Youbi, N., Admou, H., Saquaque, A., Boumehdi, M.A., Maacha, L., 2020. Time constraints on Early Tonian Rifting and Cryogenian Arc terrane–continent convergence along the northern margin of the West African craton: Insights from SHRIMP and LA–ICP–MS zircon geochronology in the Pan-African Anti–Atlas belt (Morocco). Gondwana Res. 85, 169–188. https://doi.org/10.1016/j.gr.2020.03.011.
El Hadi, H., Simancas, J.F., Tahiri, A., Gonzalez-Lodeiro, F., Azor, A., Martinez-Poyatos, D., 2006a. Comparative review of the Variscan granitoids of Morocco and Iberia: proposal of a broad zonation. Geodin. Acta 19, 103–116. https://doi.org/10.3166/ga.19.103-116.
El Hadi, H., Tahiri, A., Simancas Cabrera, F., González Lodeiro, F., Azor Pérez, A., Jesús Martínez Poyatos, D., 2006b. Un exemple de volcanisme calco–alcalin de type orogénique mis en place en contexte de rifting (Cambrien de l'oued Rhebar, Meseta occidentale, Maroc). Comptes Rendus Geosci. 338, 229–236. doi:10.1016/j.crte.2005.12.006.
El Hadi, H., Tahiri, A., Simancas, J.F., Lodeiro, F.G., Azor, A., Martínez Poyatos, D., 2014. Pillow lavas of Rabat northwestern Moroccan Meseta: transitional geochemical signature of magmas set up in an early Ordovician extending platform. Eurpoean J. Sci. Res. 122, 45–57.
El Haïbi, H., El Hadi, H., Pesquera, A., Tahiri, A., Martínez Poyatos, D., Zahour, G., Mehdioui, S., Tahiri, M., 2021. Geochemical and Sr–Nd isotopic constraints on the petrogenesis of the Tiflet granitoids (Northwestern Moroccan Meseta): geological implications. J. Iber. Geol. https://doi.org/10.1007/s41513-020-00156-7.
El Haibi, H., El Hadi, H., Tahiri, A., Martínez Poyatos, D., Gasquet, D., Pérez-Cáceres, I., González Lodeiro, F., Mehdioui, S., 2020. Geochronology and isotopic geochemistry of Ediacaran high–K calc–alkaline felsic volcanism: An example of a Moroccan perigondwanan (Avalonian?) remnant in the El Jadida horst (Mazagonia). J. African Earth Sci. 163, 103669 https://doi.org/10.1016/j.jafrearsci.2019.103669.
El Hassani, A., 1991. La Zone de Rabat–Tiflet: bordure nord de la Chaîne Calédono-Hercynienne du Maroc. Bull. l'Institut Sci.
El Hassani, A., Tahiri, A., Walliser, O.H., 2003. The Variscan Crust between Gondwana and Baltica. CFS Cour. Forschungsinstitut Senckenb. 81–87.
El Houicha, M., Pereira, M.F., Jouhari, A., Gama, C., Ennih, N., Fekkak, A., Ezzouhairi, H., El Attari, A., Silva, J.B., 2018. Recycling of the Proterozoic crystalline basement in the Coastal Block (Moroccan Meseta): New insights for understanding the geodynamic evolution of the northern peri–Gondwanan realm. Precambrian Res. 306, 129–154. https://doi.org/10.1016/j.precamres.2017.12.039.
Ernst, R.E., Wingate, M.T.D., Buchan, K.L., Li, Z.X., 2008. Global record of 1600–700 Ma Large Igneous Provinces (LIPs): Implications for the reconstruction of the proposed Nuna (Columbia) and Rodinia supercontinents. Precambrian Res. 160, 159–178. https://doi.org/10.1016/j.precamres.2007.04.019.
Ezzouhairi, H., Ribeiro, M.L., Ait Ayad, N., Moreira, M.E., Charif, A., Ramos, J.M.F., de Oliveira, D.P.S., Coke, C., 2008. The magmatic evolution at the Moroccan outboard of the West African craton between the Late Neoproterozoic and the Early Palaeozoic. Geol. Soc. London. Spec. Publ. 297, 329–343. https://doi.org/10.1144/SP297.16.
Fedo, C.M., Sircombe, K.N., Rainbird, R.H., 2003. Detrital Zircon Analysis of the Sedimentary Record. Rev. Mineral. Geochemistry 53, 277–303. https://doi.org/10.2113/0530277.
Fernández-Suárez, J., Gutiérrez-Alonso, G., Pastor-Galán, D., Hofmann, M., Murphy, J.B., Linnemann, U., 2014. The Ediacaran-Early Cambrian detrital zircon record of NW Iberia: Possible sources and paleogeographic constraints. Int. J. Earth Sci. 103, 1335–1357. https://doi.org/10.1007/s00531-013-0923-3.
Franke, W., Cocks, L.R.M., Torsvik, T.H., 2017. The Palaeozoic Variscan oceans revisited. Gondwana Res. 48, 257–284. https://doi.org/10.1016/j.gr.2017.03.005.
Franke, W., Dulce, J.-C., 2017. Back to sender: tectonic accretion and recycling of Baltica–derived Devonian clastic sediments in the Rheno-Hercynian Variscides. Int. J. Earth Sci. 106, 377–386. https://doi.org/10.1007/s00531-016-1408-y.
Gärtner, A., Youbi, N., Villeneuve, M., Linnemann, U., Sagawe, A., Hofmann, M., Zieger, J., Mahmoudi, A., Boumehdi, M.A., 2018. Provenance of detrital zircon from siliciclastic rocks of the Sebkha Gezmayet unit of the Adrar Souttouf Massif (Moroccan Sahara) – Palaeogeographic implications. Comptes Rendus – Geosci. 350, 255–266. https://doi.org/10.1016/j.crte.2018.06.004.
Gärtner, A., Youbi, N., Villeneuve, M., Sagawe, A., Hofmann, M., Mahmoudi, A., Boumehdi, M.A., Linnemann, U., 2017. The zircon evidence of temporally changing sediment transport—the NW Gondwana margin during Cambrian to Devonian time (Aoucert and Smara areas, Moroccan Sahara). Int. J. Earth Sci. 106, 2747–2769. https://doi.org/10.1007/s00531-017-1457-x.
Gasquet, D., Chevremont, P., Baudin, T., Chalot-Prat, F., Guerrot, C., Cocherie, A., Roger, J., Hassenforder, B., Cheilletz, A., 2004. Polycyclic magmatism in the Tagragra d'Akka and Kerdous-Tafeltast inliers (Western Anti-Atlas, Morocco). J. African Earth Sci. 39, 267–275. https://doi.org/10.1016/j.jafrearsci.2004.07.062.
Gehrels, G., 2012. Detrital Zircon U–Pb Geochronology: Current Methods and New Opportunities, in: Busby, C.J., Azor, A. (Eds.), Tectonics of Sedimentary Basins. John Wiley & Sons, Ltd, Chichester, UK, pp. 45–62. doi:10.1002/9781444347166.ch2.
Ghienne, J.F., Benvenuti, A., El Houicha, M., Girard, F., Kali, E., Khoukhi, Y., Langbour, C., Magna, T., Míková, J., Moscariello, A., Schulmann, K., 2018. The impact of the end–Ordovician glaciation on sediment routing systems: A case study from the Meseta (northern Morocco). Gondwana Res. 63, 169–178. https://doi.org/10.1016/j.gr.2018.07.001.
Gutiérrez-Alonso, G., Fernández-Suárez, J., Pastor-Galán, D., Johnston, S.T., Linnemann, U., Hofmann, M., Shaw, J., Colmenero, J.R., Hernández, P., 2015. Significance of detrital zircons in Siluro-Devonian rocks from Iberia. J. Geol. Soc. London. 172, 309–322. https://doi.org/10.1144/jgs2014-118.
Hefferan, K., Soulaimani, A., Samson, S.D., Admou, H., Inglis, J., Saquaque, A., Latifa, C., Heywood, N., 2014. A reconsideration of Pan African orogenic cycle in the Anti-Atlas Mountains. Morocco. J. African Earth Sci. 98, 34–46. https://doi.org/10.1016/j.jafrearsci.2014.03.007.
Hirdes, W., Davis, D.W., Eisenlohr, B.N., 1992. Reassessment of Proterozoic granitoid ages in Ghana on the basis of U/Pb zircon and monazite dating. Precambrian Res. 56, 89–96. https://doi.org/10.1016/0301-9268(92)90085-3.
Hoepffner, C., 1989. L'évolution structurale hercynienne de la Méséta marocain orientale. Essai de mise au point. Notes Mem. du Serv, Géologique du Maroc.
Hoepffner, C., 1987. La tectonique hercynienne dans l'Est du Maroc. Université Louis Pasteur, Strasbourg.
Hoepffner, C., 1977. Données nouvelles sur le Paléozoïques de la bordure occidentale du massif du Tazekka. Comptes Rendus l'Académie des Sci. Paris 284, 1635–1637.
Hoepffner, C., Houari, M.R., Bouabdelli, M., 2006. Tectonics of the North African Variscides (Morocco, western Algeria): An outline. Comptes Rendus – Geosci. 338, 25–40. https://doi.org/10.1016/j.crte.2005.11.003.
Hoepffner, C., Soulaimani, A., Piqué, A., 2005. The Moroccan Hercynides. J. African Earth Sci. 43, 144–165. https://doi.org/10.1016/j.jafrearsci.2005.09.002.

Horon, O., 1952. Contribution a l'étude du bassin de Djerada. Notes Mem. du Prot. la Repub. Française au Maroc 89, 180.
Hurley, P.M., Leo, G.W., White, R.W., Fairbairn, H.W., 1971. Liberian age province (about 2,700 m.y.) and adjacent provinces in Liberia and Sierra Leone. GSA Bull. 82, 3483–3490. https://doi.org/10.1130/0016-7606(1971)82[3483:LAPAMA]2.0.CO;2.
Iizuka, T., Yamaguchi, T., Hibiya, Y., Amelin, Y., 2015. Meteorite zircon constraints on the bulk Lu–Hf isotope composition and early differentiation of the Earth. Proc. Natl. Acad. Sci. U. S. A. 112, 5331–5336. https://doi.org/10.1073/pnas.1501658112.
Kaiser, S.I., Becker, R.T., El Hassani, A., 2007. Middle to Late Famennian successions at Ain Jemaa (Moroccan Meseta) - Implications for regional correlation, event stratigraphy and synsedimentary tectonics of NW Gondwana. Geol. Soc. Spec. Publ. 278, 237–260. https://doi.org/10.1144/SP278.11.
Kharbouch, F., 1994. Le volcanisme dévono–dinantien du Massif central et de la Meseta orientale. Bull. l'Institut Sci. Rabat 18, 192–200.
Kharbouch, F., Juteau, T., Treuil, M., Joron, J.-L., Piqué, A., Hoepffner, C., 1985. Le volcanisme dinantien de la Meseta marocaine nord–occidentale et orientale. Caractères pétrographiques et géochimiques et implications géodynamiques. Sci. Gèol. Bull. 38, 155–163.
Košler, J., Konopásek, J., Sláma, J., Vrána, S., 2014. U-Pb zircon provenance of Moldanubian metasediments in the Bohemian Massif. J. Geol. Soc. London. 171, 83–95. https://doi.org/10.1144/jgs2013-059.
Kuiper, Y.D., 2019. An overview of middle to late Paleozoic connections between southeastern New England, USA, and Morocco. Eos Transactions. American Geophysical Union, Fall Meeting.
Kuiper, Y.D., Michard, A., Ruellan, E., Holm-Denoma, C., Crowley, J.L., 2019. U-Pb zircon and monazite results from granite and charnockite from the Mazagan escarpment, offshore Morocco, in: GSA Abstracts with Programs Vol. 51, No. 2.
Kuiper, Y.D., Michard, A., Ruellan, E., Holm-Denoma, C., Crowley, J.L., 2021. New petrographic and U-Pb geochronology data from the Mazagan Escarpment, offshore Morocco: support for an African origin. Journal of African Earth Sciences 181. https://doi.org/10.1016/j.jafrearsci.2021.104249.
Lama, C., Zimmermann, J.L., Mortaji, A., Macaudière, J., Stussi, J.M., 1993. Age K-Ar protérozoïque moyen des leucogranites à deux micas de la Tagragra d'Akka (Anti Atlas occidental, Maroc). Comptes Rendus l'Académie des Sci. Paris 317, 1601–1607.
Letsch, D., El Houicha, M., von Quadt, A., Winkler, W., 2018. A missing link in the peri–Gondwanan terrane collage: The Precambrian basement of the Moroccan Meseta and its lower Paleozoic cover. Can. J. Earth Sci. 55, 33–51. https://doi.org/10.1139/cjes-2017-0086.
Liégeois, J.P., Claessens, W., Camara, D., Klerkx, J., 1991. Short–lived Eburnian orogeny in southern Mali. Geology, tectonics, U-Pb and Rb–Sr geochronology. Precambrian Res. 50, 111–136.
Lin, W., Faure, M., Li, X.-H., Ji, W., 2019. Pre-Variscan tectonic setting of the south margin of Armorica: Insights from detrital zircon ages distribution and Hf isotopic composition of the St–Georges–sur–Loire Unit (S. Armorican Massif, France). Tectonophysics 766, 340–378. https://doi.org/10.1016/j.tecto.2019.06.015.
Lin, W., Faure, M., Li, X. hua, Chu, Y., Ji, W., Xue, Z., 2016. Detrital zircon age distribution from Devonian and Carboniferous sandstone in the Southern Variscan Fold–and–Thrust belt (Montagne Noire, French Massif Central), and their bearings on the Variscan belt evolution. Tectonophysics 677–678, 1–33. doi:10.1016/j.tecto.2016.03.032.
Linnemann, U., Gerdes, A., Drost, K., Buschmann, B., 2007. The continuum between Cadomian orogenesis and opening of the Rheic Ocean: Constraints from LA–ICP–MS U–Pb zircon dating and analysis of plate–tectonic setting (Saxo–Thuringian zone, northeastern Bohemian Massif, Germany), in: The Evolution of the Rheic Ocean: From Avalonian–Cadomian Active Margin to Alleghenian–Variscan Collision. Geological Society of America, pp. 61–96. doi:10.1130/2007.2423(03).
Linnemann, U., McNaughton, N.J., Romer, R.L., Gehmlich, M., Drost, K., Tonk, C., 2004. West African provenance for Saxo-Thuringia (Bohemian Massif): did Armorica ever leave pre–Pangean Gondwana? – U/Pb–SHRIMP zircon evidence and the Nd–isotopic record. Int. J. Earth Sci. 93, 683–705. https://doi.org/10.1007/s00531-004-0413-8.
Linnemann, U., Ouzegane, K., Drareni, A., Hofmann, M., Becker, S., Gärtner, A., Sagawe, A., 2011. Sands of West Gondwana: An archive of secular magmatism and plate interactions – A case study from the Cambro-Ordovician section of the Tassili Ouan Ahaggar (Algerian Sahara) using U-Pb–LA–ICP–MS detrital zircon ages. Lithos 123, 188–203. https://doi.org/10.1016/j.lithos.2011.01.010.
Linnemann, U., Pereira, M.F., Jeffries, T.E., Drost, K., Gerdes, A., 2008. The Cadomian Orogeny and the opening of the Rheic Ocean: The diacrony of geotectonic processes constrained by LA–ICP–MS U-Pb zircon dating (Ossa–Morena and Saxo-Thuringian Zones, Iberian and Bohemian Massifs). Tectonophysics 461, 21–43. https://doi.org/10.1016/j.tecto.2008.05.002.
Ludwig, K.R., 2003. Isoplot 3.0. A geochronological toolkit for Microsoft Excel. Berkeley Geochron, Cent. Spec. Publ. 4, 70.
Marhoumi, M.R., Doubinger, J., Rauscher, R., Hoepffner, C., 1989. Données nouvelles sur le Paléozoïque de la Méséta oriental marocaine. Apports de la palynologie. Notes Mem. du Serv, Géologique du Maroc.
Matte, P., 2001. The Variscan collage and orogeny (480–290 Ma) and the tectonic definition of the Armorica microplate: a review. Terra Nov. 13, 122–128. https://doi.org/10.1046/j.1365-3121.2001.00327.x.
Médioni, R., 1979. Carte géologique du Maroc au 1/100.000. Feuille Hassiane Ed Diab. Notice explicative. Notes Mem. du Serv. Géologique du Maroc 227, 64.
Meinhold, G., Morton, A.C., Avigad, D., 2013. New insights into peri-Gondwana paleogeography and the Gondwana super-fan system from detrital zircon U-Pb ages. Gondwana Res. 23, 661–665. https://doi.org/10.1016/j.gr.2012.05.003.
Meinhold, G., Morton, A.C., Fanning, C.M., Frei, D., Howard, J.P., Phillips, R.J., Strogen, D., Whitham, A.G., 2011. Evidence from detrital zircons for recycling of Mesoproterozoic and Neoproterozoic crust recorded in Paleozoic and Mesozoic sandstones of southern Libya. Earth Planet. Sci. Lett. 312, 164–175. https://doi.org/10.1016/j.epsl.2011.09.056.
Michard, A., 1976. Éléments de géologie marocaine. Notes Mem. du Serv. Géologique du Maroc 252, 408.
Michard, A., Cailleux, Y., Hoepffner, C., 1989. L'orogène mésétien du Maroc: structure, déformation hercynienne et déplacement. Notes Mem. du Serv, Géologique du Maroc.
Michard, A., Ouanaimi, H., Hoepffner, C., Soulaimani, A., Baidder, L., 2010a. Comment on Tectonic relationships of Southwest Iberia with the allochthons of Northwest Iberia and the Moroccan Variscides by J.F. Simancas et al. [C. R. Geoscience 341 (2009) 103–113]. Comptes Rendus – Geosci. 342, 170–174. doi:10.1016/j.crte.2010.01.008.
Michard, A., Soulaimani, A., Hoepffner, C., Ouanaimi, H., Baidder, L., Rjimati, E.C., Saddiqi, O., 2010. The South-Western Branch of the Variscan Belt: evidence from Morocco. Tectonophysics 492, 1–24. https://doi.org/10.1016/j.tecto.2010.05.021.
Montero, P., Talavera, C., Bea, F., Lodeiro, F.G., Whitehouse, M.J., 2009. Zircon Geochronology of the Ollo de Sapo Formation and the Age of the Cambro-Ordovician Rifting in Iberia. J. Geol. 117, 174–191. https://doi.org/10.1086/595017.
Morin, P., 1960. Les marbres d'origine métamorphique du Maroc central (géologie et problèmes d'exploitation). Mines et géologie 11, 559–574.
Muratet, B., 1995. Carte géologique du Maroc No364: Taourirt – Echelle 1/100.000. Roy. du Maroc, Ministère l'Energie des Mines du Développement Durable.
Nance, R.D., Gutiérrez-Alonso, G., Keppie, J.D., Linnemann, U., Murphy, J.B., Quesada, C., Strachan, R.A., Woodcock, N.H., 2012. A brief history of the Rheic Ocean. Geosci. Front. 3, 125–135. https://doi.org/10.1016/j.gsf.2011.11.008.
Nance, R.D., Gutiérrez-Alonso, G., Keppie, J.D., Linnemann, U., Murphy, J.B., Quesada, C., Strachan, R.A., Woodcock, N.H., 2010. Evolution of the Rheic Ocean. Gondwana Res. 17, 194–222. https://doi.org/10.1016/j.gr.2009.08.001.
D'lemos, R., Pisarevsky, S.A., 2008. Neoproterozoic–early Palaeozoic tectonostratigraphy and palaeogeography of the peri–Gondwanan terranes: Amazonian v. West African connections. Geol. Soc. London, Spec. Publ. 297, 345–383. doi:10.1144/SP297.17.
Ouabid, M., Garrido, C.J., Ouali, H., Harvey, J., Hidas, K., Marchesi, C., Acosta-Vigil, A., Dautria, J., El Messbahi, H., Román-Alpiste, M.J., 2020. Late Cadomian rifting of the NW Gondwana margin and the reworking of Precambrian crust – evidence from bimodal magmatism in the early Paleozoic Moroccan Meseta. Int. Geol. Rev. 00, 1–24. https://doi.org/10.1080/00206814.2020.1818301.
Ouabid, M., Ouali, H., Garrido, C.J., Acosta-Vigil, A., Román-Alpiste, M.J., Dautria, J.M., Marchesi, C., Hidas, K., 2017. Neoproterozoic granitoids in the basement of the Moroccan Central Meseta: Correlation with the Anti-Atlas at the NW paleo–margin of Gondwana. Precambrian Res. 299, 34–57. https://doi.org/10.1016/j.precamres.2017.07.007.
Ouali, H., Briand, B., Bouchardon, J.-L., Capiez, P., 2003. Le volcanisme cambrien du Maroc central: implications géodynamiques. Comptes Rendus Geosci. 335, 425–433. https://doi.org/10.1016/S1631-0713(03)00064-6.
Ouanaimi, H., Soulaimani, A., Hoepffner, C., Michard, A., Baidder, L., 2016. The Atlas-Meseta Red Beds basin (Morocco) and the Lower Ordovician rifting of NW–Gondwana. Bull. la Soc. Géologique Fr. 187, 155–168. https://doi.org/10.2113/gssgfbull.187.3.155.
Pastor-Galán, D., Gutiérrez-Alonso, G., Fernández-Suárez, J., Murphy, J.B., Nieto, F., 2013a. Tectonic evolution of NW Iberia during the Paleozoic inferred from the geochemical record of detrital rocks in the Cantabrian Zone. Lithos 182–183, 211–228. https://doi.org/10.1016/j.lithos.2013.09.007.
Pastor-Galán, D., Gutiérrez-Alonso, G., Murphy, J.B., Fernández-Suárez, J., Hofmann, M., Linnemann, U., 2013b. Provenance analysis of the Paleozoic sequences of the northern Gondwana margin in NW Iberia: Passive margin to Variscan collision and orocline development. Gondwana Res. 23, 1089–1103. https://doi.org/10.1016/j.gr.2012.06.015.
Pereira, M.F., Chichorro, M., Johnston, S.T., Gutiérrez-Alonso, G., Silva, J.B., Linnemann, U., Hofmann, M., Drost, K., 2012. The missing Rheic Ocean magmatic arcs: provenance analysis of Late Paleozoic sedimentary clastic rocks of SW Iberia. Gondwana Res. 22, 882–891. https://doi.org/10.1016/j.gr.2012.03.010.
Pereira, M.F., El Houicha, M., Chichorro, M., Armstrong, R., Jouhari, A., El Attari, A., Ennih, N., Silva, J.B., 2015. Evidence of a Paleoproterozoic basement in the Moroccan Variscan Belt (Rehamna Massif, Western Meseta). Precambrian Res. 268, 61–73. https://doi.org/10.1016/j.precamres.2015.07.010.
Pereira, M.F., Gutíerrez-Alonso, G., Murphy, J.B., Drost, K., Gama, C., Silva, J.B., 2017. Birth and demise of the Rheic Ocean magmatic arc(s): Combined U-Pb and Hf isotope analyses in detrital zircon from SW Iberia siliciclastic strata. Lithos 278–281, 383–399. https://doi.org/10.1016/j.lithos.2017.02.009.
Pérez-Cáceres, I., Martínez Poyatos, D., Simancas, J.F., Azor, A., 2017. Testing the Avalonian affinity of the South Portuguese Zone and the Neoproterozoic evolution of SW Iberia through detrital zircon populations. Gondwana Res. 42, 177–192. https://doi.org/10.1016/j.gr.2016.10.010.
Perez, N.D., Teixell, A., Gómez-Gras, D., Stockli, D.F., 2019. Reconstructing Extensional Basin Architecture and Provenance in the Marrakech High Atlas of Morocco: Implications for Rift Basins and Inversion Tectonics. Tectonics 38, 1584–1608. https://doi.org/10.1029/2018TC005413.
Pique, A., 1994. Introduction historique et structurale. (Le Massif central marocain et la Meseta oriental). Bull. l'Institut Sci. Rabat 18, 1–2.
Piqué, A., 2003. Evidence for an important extensional event during the Latest Proterozoic and Earliest Paleozoic in Morocco. Comptes Rendus Geosci. 335, 865–868. https://doi.org/10.1016/j.crte.2003.08.005.

Piqué, A., 2001. Geology of Northwest Africa. Gebrüder Borntraeger, Berlin.
Piqué, A., 1994. Géologie du Maroc. éditions Pumag, Marrakech.
Piqué, A., 1981. La chaîne hercynienne d'Europe occidentale et son prolongement dans le Nord-Ouest de l'Afrique. Sci. Géologiques. Bull. 34, 123–134. https://doi.org/10.3406/sgeol.1981.1596.
Piqué, A., 1979. Évolution structurale d'un segment de la chaîne hercynienne: la Meseta marocaine nord–occidentale. Ph.D. Thesis. Université de Strasbourg.
Piqué, A., Bouabdelli, M., Darboux, J.-R., 1995. Le rift cambrien du Maroc occidental. Comptes Rendus l'Académie des Sci. – Ser. IIA – Earth Planet. Sci. 320, 1017–1024.
Piqué, A., Michard, A., 1989. Moroccan Hercynides: a synopsis. The Paleozoic sedimentary and tectonic evolution at the northern margin of West Africa. Am. J. Sci. 289, 286–330.
Pouclet, A., El Hadi, H., Álvaro, J.J., Bardintzeff, J.-M., Benharref, M., Fekkak, A., 2018. Review of the Cambrian volcanic activity in Morocco: geochemical fingerprints and geotectonic implications for the rifting of West Gondwana. Int. J. Earth Sci. 107, 2101–2123. https://doi.org/10.1007/s00531-018-1590-1.
Rauscher, R., Marhoumi, M.R., Vanguestaine, M., Hoepffner, C., 1982. Datation palynologique des schistes du Tazekka au Maroc. Hypothèse structurale sur la socle hercynien de la Meseta orientale. Comptes Rendus l'Académie des Sci. Paris 294, 1203–1206.
Razin, P., Janjou, D., Baudin, T., Bensahal, A., Hoepffner, C., Chenakeb, M., Cailleux, Y., 2001. Carte géologique du Maroc No412: Sidi Matla' Ech Chams – Echelle 1/50.000. Roy. du Maroc, Ministère l'Energie des Mines du Développement Durable.
Sánchez–García, T., Bellido, F., Quesada, C., 2003. Geodynamic setting and geochemical signatures of Cambrian–Ordovician rift–related igneous rocks (Ossa–Morena Zone, SW Iberia). Tectonophysics 365, 233–255. doi:10.1016/S0040–1951(03)00024–6.
Sánchez–García, T., Chichorro, M., Solá, A.R., Álvaro, J.J., Díez–Montes, A., Bellido, F., Ribeiro, M.L., Quesada, C., Lopes, J.C., Dias da Silva, I., González–Clavijo, E., Gómez Barreiro, J., López–Carmona, A., 2019. The Cambrian–Early Ordovician Rift Stage in the Gondwanan Units of the Iberian Massif. In: Quesada, C., Oliveira, J.T. (Eds.), The Geology of Iberia: A Geodynamic Approach, Regional Geology Reviews. Springer, pp. 27–74. https://doi.org/10.1007/978–3–030–10519–8_2.
Schofield, D.I., Horstwood, M.S.A., Pitfield, P.E.J., Crowley, Q.G., Wilkinson, A.F., Sidaty, H.C.O., 2006. Timing and kinematics of Eburnean tectonics in the central Reguibat Shield. Mauritania. J. Geol. Soc. London. 163, 549–560. https://doi.org/10.1144/0016-764905-097.
Sharman, G.R., Malkowski, M.A., 2020. Needles in a haystack: Detrital zircon U Pb ages and the maximum depositional age of modern global sediment. Earth-Science Rev. 203, 103–109. https://doi.org/10.1016/j.earscirev.2020.103109.
Shaw, J., Gutiérrez-Alonso, G., Johnston, S.T., Pastor Galán, D., 2014. Provenance variability along the Early Ordovician north Gondwana margin: Paleogeographic and tectonic implications of U-Pb detrital zircon ages from the Armorican Quartzite of the Iberian Variscan belt. Bull. Geol. Soc. Am. 126, 702–719. https://doi.org/10.1130/B30935.1.
Simancas, J.F., Azor, A., Martínez-Poyatos, D., Tahiri, A., El Hadi, H., González-Lodeiro, F., Pérez-Estaún, A., Carbonell, R., 2009. Tectonic relationships of Southwest Iberia with the allochthons of Northwest Iberia and the Moroccan Variscides. Comptes Rendus Geosci. 341, 103–113. https://doi.org/10.1016/j.crte.2008.11.003.
Simancas, J.F., Azor, A., Martínez–Poyatos, D., Tahiri, A., Hadi, H. El, González–Lodeiro, F., Pérez–Estaún, A., Carbonell, R., 2010. Reply to the comment by Michard et al. on "Tectonic relationships of Southwest Iberia with the allochthons of Northwest Iberia and the Moroccan Variscides." Comptes Rendus – Geosci. 342, 175–177. doi:10.1016/j.crte.2010.01.007.
Simancas, J.F., Tahiri, A., Azor, A., Lodeiro, F.G., Martínez Poyatos, D.J., El Hadi, H., 2005. The tectonic frame of the Variscan-Alleghanian orogen in Southern Europe and Northern Africa. Tectonophysics 398, 181–198. https://doi.org/10.1016/j.tecto.2005.02.006.
Spencer, C.J., Kirkland, C.L., Taylor, R.J.M., 2016. Strategies towards statistically robust interpretations of in situ U-Pb zircon geochronology. Geosci. Front. 7, 581–589. https://doi.org/10.1016/j.gsf.2015.11.006.
Strnad, L., Mihaljevič, M., 2005. Sedimentary provenance of Mid–Devonian clastic sediments in the Teplá–Barrandian Unit (Bohemian Massif): U–Pb and Pb–Pb geochronology of detrital zircons by laser ablation ICP–MS. Mineral. Petrol. doi:10.1007/s00710–004–0057–1.
Szczepański, J., Turniak, K., Anczkiewicz, R., Gleichner, P., 2020. Dating of detrital zircons and tracing the provenance of quartzites from the Bystrzyckie Mts: implications for the tectonic setting of the Early Palaeozoic sedimentary basin developed on the Gondwana margin. Int. J. Earth Sci. 109, 2049–2079. https://doi.org/10.1007/s00531-020-01888-8.
Tahiri, A., 1994. Tectonique hercynienne de l'anticlinorium de Khouribga-Oulmès et du synclinorium de Fourhal. Bull. l'Institut Sci. Rabat 18, 125–144.
Tahiri, A., 1991. Le Maroc central septentrional: stratigraphie, sedimentologie et tectonique du Paleozoïque; un exemple de passage des zones internes aux zones externes de la chaïne Hercynienne du Maroc. Ph.D. Thesis. Université de Bretagne Occidentale, Brest, France.
Tahiri, A., El Hassani, A., 1994. L'Ordovicien du Maroc central septentrional. Bull. l'Institut Sci. Rabat 18, 32–37.
Tahiri, A., Montero, P., El Hadi, H., Martínez Poyatos, D., Azor, A., Bea, F., Simancas, J. F., González Lodeiro, F., 2010. Geochronological data on the Rabat-Tiflet granitoids: their bearing on the tectonics of the Moroccan Variscides. J. African Earth Sci. 57, 1–13. https://doi.org/10.1016/j.jafrearsci.2009.07.005.
Talavera, C., Montero, P., Martínez Poyatos, D., Williams, I.S., 2012. Ediacaran to Lower Ordovician age for rocks ascribed to the Schist-Graywacke Complex (Iberian Massif, Spain): Evidence from detrital zircon SHRIMP U-Pb geochronology. Gondwana Res. 22, 928–942. https://doi.org/10.1016/j.gr.2012.03.008.
Vermeesch, P., 2012. On the visualisation of detrital age distributions. Chem. Geol. 312–313, 190–194. https://doi.org/10.1016/j.chemgeo.2012.04.021.
Vermeesch, P., 2004. How many grains are needed for a provenance study? Earth Planet. Sci. Lett. 224, 441–451. https://doi.org/10.1016/j.epsl.2004.05.037.
Verset, Y., 1985. Carte géologique du Maroc: feuille N° 340 Qasbat-Tadla, Echelle 1/100.000. Service Géologique du Maroc.
Verset, Y., 1988. Mémoire explicatif de la carte géologique du Maroc au 1:100.000, feuille de Qasbat-Tadla. Notes Mem. du Serv. Géologique du Maroc.
Vidal, J.C., Hoepffner, C., 1979. Carte géologique du Rif No282: Tahala – Echelle 1/50.000. Roy. du Maroc, Ministère l'Energie des Mines du Développement Durable.
Villeneuve, M., El Archi, A., Nzamba, J., 2010. Les chaînes de la marge occidentale du Craton Ouest-Africain, modèles géodynamiques. Comptes Rendus – Geosci. 342, 1–10. https://doi.org/10.1016/j.crte.2009.12.002.
Walliser, O.H., El Hassani, A., Tahiri, A., 2000. Mrirt: a key area for the Variscan Meseta of Morocco. Notes Mémoires du Serv. Géologique du Maroc 399, 93–108.
Walliser, O.H., El Hassani, A., Tahiri, A., 1995. Sur le Dévonien de la Meseta marocaine occidentale. Comparaisons avec le Dévonien allemand et évènements globaux. CFS Cour. Forschungsinstitut Senckenb. 188, 21–30.
Youbi, N., Kouyaté, D., Söderlund, U., Ernst, R.E., Soulaimani, A., Hafid, A., Ikenne, M., El Bahat, A., Bertrand, H., Rkha Chaham, K., Ben Abbou, M., Mortaji, A., El Ghorfi, M., Zouhair, M., El Janati, M., 2013. The 1750Ma Magmatic Event of the West African Craton (Anti–Atlas, Morocco). Precambrian Res. 236, 106–123. https://doi.org/10.1016/j.precamres.2013.07.003.
Zahraoui, M., 1994. Le Silurien. Bull. l'Institut Sci. Rabat 18, 38–42.
Žák, J., Sláma, J., 2018. How far did the Cadomian 'terranes' travel from Gondwana during early Palaeozoic? A critical reappraisal based on detrital zircon geochronology. Int. Geol. Rev. 60, 319–338. doi:10.1080/00206814.2017.1334599.